Electrospun PCL-Ascorbic Acid Fibres as Antioxidant Cardiac Tissue Scaffolds

Ella-Louise Handley, Anthony Callanan

Institute for Bioengineering, School of Engineering, University of Edinburgh, Scotland, UK

INTRODUCTION: Cardiovascular diseases are the leading cause of death globally, of which myocardial infarction (MI) is responsible for the largest portion of deaths[1]. In recent years, MI has accounted for over 160,000 hospital admissions annually in the UK[2]. Current treatments for MI are limited due to the poor regenerative capabilities of the heart; whilst tissue engineering holds great promise for repair of the myocardium, the harsh hypoxic tissue results in low efficacy of regenerative treatments, thus recent research has been focusing on methods to rejuvenate the microenvironment. One such method is by using an antioxidant to scavenge overproduced reactive oxygen species (ROS), which are known to trigger cell apoptosis via damage of proteins, lipids and nucleic acids[3]. In this study, L-ascorbic acid (AA) was incorporated into electrospun PCL fibres with the aim to support cell growth whilst reversing the oxidative microenvironment.

METHODS: PCL scaffolds were electrospun with two different concentrations of AA. The AA was homogenised in HFIP and PCL added, and the solutions were continuously stirred overnight. The test groups were 10w/v% PCL + 0.1w/v% AA in HFIP and 10w/v% PCL + 0.05w/v% AA in HFIP; the control scaffold was 10w/v% PCL in HFIP. Scaffolds were fabricated using electrospinning techniques to create mats with randomly aligned fibres. These were characterised using SEM imaging and mechanical testing (Instron 3367). The antioxidant capabilities of the scaffold were measured using hydrogen peroxide and DPPH assays. Vascular cells were cultured on the scaffolds under normal and oxidative conditions, and the cytotoxicity and viability were determined at different timepoints.

RESULTS: Three scaffolds with similar morphology and mechanical properties incorporating varying concentrations of AA were successfully fabricated via electrospinning. Results of the two antioxidant assays confirm the scaffolds have increased antioxidant capabilities compared to the control. Scaffolds supported the survival and proliferation of cells.

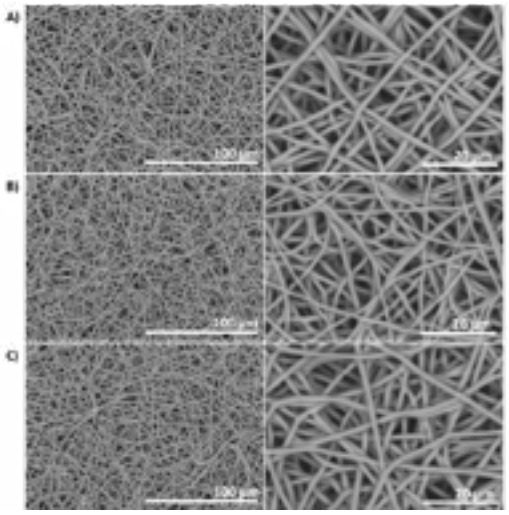

Fig. 1: SEM images of the A) control B) 0.05% and C) 0.1% scaffolds.

Table 1. Fibre diameter and mechanical testing data

	PCL Control	0.05% AA	0.1% AA
Fibre Diameter (µm)	1.696 ± 0.124	1.336 ± 0.153	1.654 ± 0.119
Young's Modulus (0-5% strain) (MPa)	4.194 ± 0.650	2.285 ± 0.196	3.235 ± 0.218
Young's Modulus (5-10% strain) (MPa)	2.078 ± 0.293	1.026 ± 0.140	1.361 ± 0.192

DISCUSSION & CONCLUSIONS: Results showed that the incorporation of AA into electrospun PCL fibres is capable of scavenging ROS in an oxidative environment and maintaining cell viability. This study provides motivation for further investigation into the inclusion of antioxidant vitamins in cardiac scaffolds and how this can be optimised to further reverse the harsh microenvironment of the post-infarcted tissue.

ACKNOWLEDGEMENTS: This work is funded by an EPSRC grant EP/T517884/1 and and MRC grant MR/L012766/1.

REFERENCES: [1]WHO. CVDs, Fact Sheets, (2017), [2]NHS Digital. Hospital Admitted Patient Care Activity 2019-20 (2020), [3]Redza-Dutordoir, M. Biochimica et Biophysica Act **1863**, 2977-2992 (2016).

The effect of Geranylgeraniol (GGOH) on zoledronate-induced toxicity on oral fibroblasts and keratinocytes.

K. Rattanawonsakul[1], F. Claeyssens[1], R. Bolt[2], S. Atkins[2], V. Hearnden[1]

[1]*Department of Materials Science and Engineering, Kroto Research Institute, University of Sheffield, S3 7HQ, Sheffield, GB*

[2]*School of Clinical Dentistry, University of Sheffield, S10 2TA, Sheffield, GB*

INTRODUCTION: Bisphosphonate therapies for the treatment of bone-related cancer are associated with the development of medication-related osteonecrosis of the jaw (MRONJ)[1]. The disease is presented with an exposure of necrotic bone with soft tissue wounds in the oral cavity[2]. The pathogenesis and definitive treatment strategies have yet been concluded. Nitrogen-containing bisphosphonates (N-BPs) such as zoledronate (ZA) or pamidronate (PA) primarily inhibit bone resorption through the mevalonate pathway by reducing geranylated proteins which are essential for osteoclast activities[3]. The toxicity of BPs also impairs oral soft tissue healing[2]. Geranylgeraniol (GGOH), a derivative of geranylated substance, has been able to counteract ZA toxicity in osteoclasts[4]. This study aimed to investigate the in vitro effect of GGOH on ZA-induced toxicity in oral mucosa cells.

METHODS: Primary oral fibroblasts (NOFs) and keratinocytes (NOKs) isolated from buccal mucosa were used in this study. Cells were incubated with five GGOH concentrations from 0.5 to 10 µM or GGOH in combination with 10 µM ZA for 72 hours. Cellular viability was analysed using an MTT assay. Absorbance was read at 542/630 nm.

RESULTS: All GGOH concentrations had no significant toxic effect on the cell viability after 72 hours of treatment (Data not shown for 0.5 – 5 µM GGOH). ZA markedly lowered the metabolic activities NOKs. GGOH showed a slight recovery in the viability of both cells in the presence of ZA in a dose-dependent manner however this did not reach statistical significance.

DISCUSSION & CONCLUSIONS: GGOH produced no cytotoxicity towards oral fibroblasts and keratinocytes. There was no apparent effect of GGOH on reversing ZA-induced toxicity when studying the viability of oral mucosa cells. Future studies using PA or higher GGOH doses should be done to confirm the efficacy of GGOH and its potential to be used for MRONJ management.

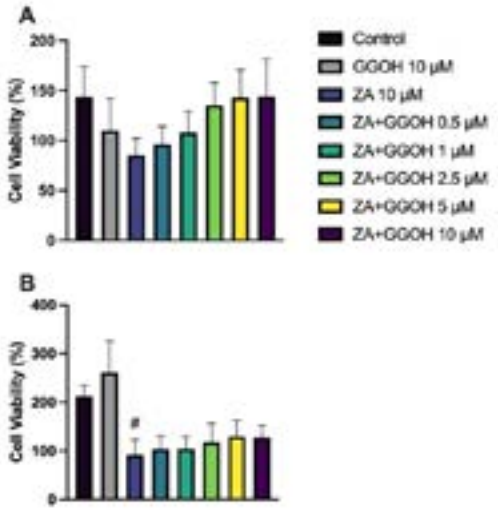

Figure 1 The viability of (A) primary oral fibroblasts and (B) oral keratinocytes after treated with 10 µM ZA in combination with different GGOH concentrations for 72 hours. (#) indicates statistical significance ($p \leq 0.05$) when compared to controls

ACKNOWLEDGEMENTS: We would like to thank Dr. George Bullock and Mrs Vanessa Singleton for laboratory support, Dr. Helen Colley for the support in obtaining primary cells. This project was funded Faculty of Dentistry, Mahidol University, Thailand.

REFERENCES:

1. Cozin M. et al. *J Oral Maxillofac Surg*. 2011;69(10):2564-2578.
2. Ruggiero SL. et al. A *J Oral Maxillofac Surg*. 2014;72(10):1938-1956.
3. Kumar V, Sinha RK. *J Maxillofac Oral Surg*. 2014;13(4):386-393.
4. Fliefel RM et al. S. *Stem Cells Int*. 2019;2019

Engineered neural tissue made using clinical-grade human neural stem cells supports regeneration in a critical gap-length nerve injury.

Melissa LD Rayner [1,2], Adam GE Day [1,2], Kulraj S Bhangra[1,2], John Sinden [1,2] and James B Phillips [1,2].

[1] School of Pharmacy, UCL, London, UK. [2] UCL Centre for Nerve Engineering, London, UK.

INTRODUCTION: A surgical autograft remains the clinical gold-standard therapy for gap repair following peripheral nerve injury, however, challenges remain with achieving full recovery and reducing donor-site morbidity [1]. Engineered neural tissue manufactured using human stem cells [2] (EngNT-CTX) has been developed as a potential 'off the shelf' allogeneic autograft replacement.

METHODS: The effectiveness of EngNT-CTX (Fig 1) was compared to an autograft in a critical length gap sciatic nerve injury model in athymic rats. Outcome measures assessed neuronal regeneration and functional recovery.

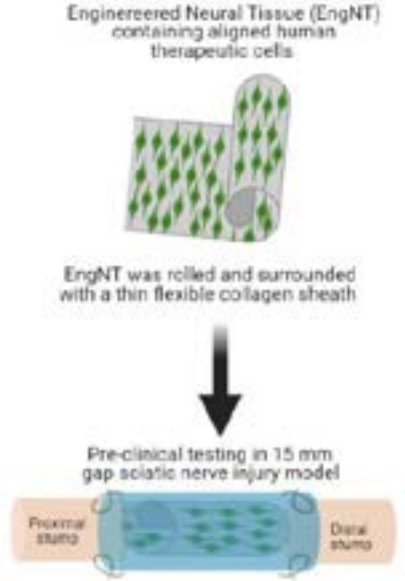

Fig 1: Representative images of the manufactured EngNT-CTX and surgical implantation in vivo.

RESULTS: At both 8 and 16 weeks, EngNT-CTX restored electrophysiological nerve conduction and functional reinnervation of downstream muscles to the same extent as the autograft. Histological analysis confirmed that more motor neurons had successfully regenerated through the repair with EngNT-CTX in comparison to the autograft at 8 weeks (Fig 2B), which was consistent with the electrophysiology (Fig 2A). The total number of neurons (motor + sensory) was greater in autografts than EngNT-CTX at 8 weeks, indicating that more sensory fibres may have sprouted in those animals at this time point.

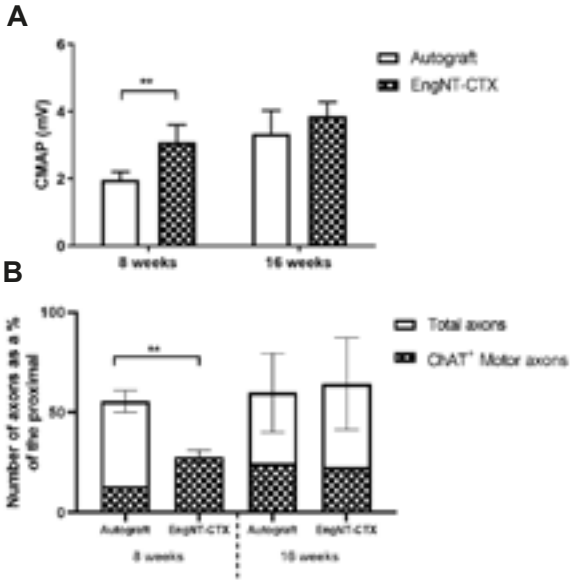

*Fig. 2: Electrophysiological analysis of the compound muscle action potential (CMAP) (A). Histological analysis of total axons in the distal stump as a percentage of the proximal and the percentage of these axons that are ChAT+ motor axons (B). n=7. Mean ± SEM. ** p<0.01.*

DISCUSSION & CONCLUSIONS: In conclusion this study provides evidence to support the effectiveness of EngNT-CTX as a replacement for the nerve autograft, as the functional regeneration assessed through histological and electrophysiological outcome measures demonstrated equivalent performance.

REFERENCES: [1] Palispis and Gupta (2017) Experimental neurology 290:106-14. [2] Pollock *et al*; (2006) Experimental neurology 199(1): 143-55.

Comparison of donor variation in human liver ECM-PCL electrospun scaffolds

Thomas Bate[1], Rhiannon Grant[2], S Ferreira-Gonzalez[3], Tak Yung Man[3], Hannah Esser[3], Gabriel Oniscu[4], Stuart Forbes[3], Anthony Callanan[1]

[1]Institute for Bioengineering, University of Edinburgh, Edinburgh, UK. [2]Maastricht University, Maastricht, Netherlands.[3]MRC Centre for Regenerative Medicine, University of Edinburgh, Edinburgh, UK. [4]The Royal Infirmary, Edinburgh, UK.

INTRODUCTION: Global mortality rates due to liver disease have increased since the 1970s, contrary to downward trends observed in other leading causes of death[1,2]. *In-vitro* drug development methods are unable to provide effective and efficient routes in which new treatments can be achieved [3]. More relevant *in-vitro* models are required to progress drug development. Electrospun scaffolds show potential for *in-vitro* research models due to the ability to mimic Extracellular Matrix (ECM) structures with biocompatible polymers and the potential of incorporating natural ECM to provide relevant biochemical cues. This study has explored the use of different human liver derived ECM (hLECM) combined with polycaprolactone (PCL) in electrospun fibres to test cell responses between liver donors.

METHODS: 1 w/w% hLECM:PCL scaffolds from five separate donors were manufactured via blending of the components within an hexafluoroisopropanol (HFIP) solvent system. Briefly, human liver tissue was decellularised via perfusion of 1% Sodium Dodecyl Sulphate (SDS) within a decellularisation system designed in-house. These were subsequently washed and lyophilised then powdered using a planetary ball mill. The powder was dissolved with 8% PCL in HFIP and electrospun into fibres. Fibres were characterized using SEM imaging, mechanical analyses, immunostaining and FTIR. Scaffolds were seeded with HepG2 cells and viability, DNA, immunofluorescence and RT-qPCR gene analysis were conducted at 24hr, 7 day and 14 day timepoints.

RESULTS: Decellularisation of the five donor tissues was confirmed by removal of DNA material. Qualitative assessment of ECM content by FTIR and histology showed differences in ECM composition between samples. Scaffolds of similar morphology were fabricated from the different samples and immunofluorescence confirmed incorporation of ECM components within the scaffolds. Support of HepG2 cultures upon the scaffolds for 14 days confirms suitability of hybrid hLECM:PCL scaffolds for hepatocyte culture. Trends in proliferative activity and expression of key hepatic functional genes were noted between groups.

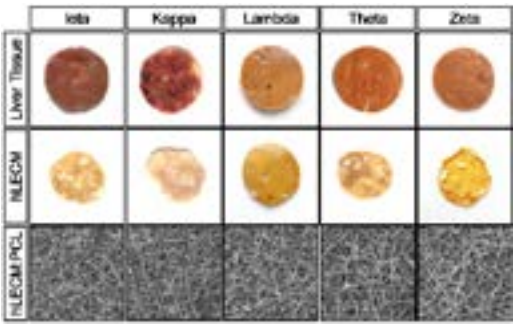

Figure 1: 5 different liver samples (top row), decellularised samples (middle row) and electrospun hLECM:PCL fibres (bottom row). Greek letters indicate different donors.

DISCUSSION & CONCLUSIONS: The incorporation of different hLECM into electrospun PCL scaffolds is capable of maintaining cell survival and inducing altered biological responses in HepG2 cells. This indicates that retained bioactive elements within the electrospun hLECM can drive hepatocyte function. Further investigation should confirm how hLECM can be classified to predict *in-vitro* responses on hLECM:PCL scaffolds. This study highlights the potential for use of different donor tissue for modelling different liver conditions.

ACKNOWLEDGEMENTS: EPSRC grant EP/N509644/1 and MRC grant MR/L012766/1. This work is enabled by the sacrifice of UK organ donors and their relatives, with the assistance of NHS ODT.

REFERENCES: [1]Tapper, E. B. BMJ **362**, k2817 (2018). [2]Williams, J. Hepatol. **63**, 297–299 (2015). [3]Hay, M., Nat. Biotechnol. **32**, 40–51 (2014).

A 3D Bioprinted Model of the Human Intervertebral Disc

S.R. Moxon[1,2,5], M. Domingos[2,3,5], J. Gough[3,4,5] & S.M. Richardson[1,2]

[1]School of Biological Sciences, University of Manchester, UK. [2]Advanced Materials in Medicine, University of Manchester, UK. [3]School of Engineering, University of Manchester, UK. [3]School of Natural Sciences, University of Manchester, UK, [5]Henry Royce Institute, University of Manchester, UK.

INTRODUCTION: The intervertebral disc (IVD) aids the flexible movement of the spinal column by providing vertebra with support against mechanical loads[1]. It is broadly comprised of two distinct tissue regions. At the core, the IVD contains a soft and gelatinous nucleus pulposus (NP) populated by spherical NP cells embedded in a polysaccharide-rich matrix. Conversely, the outer annulus fibrosus (AF) of the disc is much stiffer and comprised of elongated AF cells in an aligned, fibrous matrix[2]. Degeneration of the disc is a common problem with age being a major risk factor. Progression of IVD degeneration leads to chronic pain and can result in permanent disability. Repairing the damaged IVD is often impaired by an inability to regenerate the two distinct regions of the disc simultaneously. This study aims to investigate if a newly developed suspended hydrogel bioprinting system[3] could be employed to fabricate full-scale analogues of the IVD for tissue regeneration and disc disease modelling.

METHODS: A biphasic hydrogel construct was fabricated via suspended layer additive manufacturing (SLAM) with a 0.5% (w/w) agarose fluid gel extrusion bath. The inner 'NP-like' region was printed first with 0.25% low acyl gellan gum (Sigma, UK) as a bioink. An outer 'AF-like' region of 1% gellan gum was subsequently deposited before the entire construct was crosslinked for 60 minutes with 150 mM $CaCl_2$ (Sigma, UK). The resulting structure was extracted from the fluid gel support bath and rheologically analysed via strain sweeps (1 Hz, 37°C, γ = 0.002-0.2) using a HAAKE™ MARS™ rheometer (Thermo, UK).

RESULTS: SLAM was successfully employed to generate a single hydrogel construct with two distinct regions (Fig. 1). The resulting biphasic structure was strong enough to withstand manual handling without delamination and separation of the two gel regions. Rheological testing revealed that the central, 'NP-like' zone exhibited a considerably softer matrix stiffness than the outer 'AF' (~6 vs ~50 KPa, γ = 0.002). In both regions, the gel stiffness fell within the reported values for native tissue (NP = 1-10 KPa, AF = 50-100 KPa)[4-5]. Moreover, an interfacial region was present with a matrix stiffness of ~20 KPa.

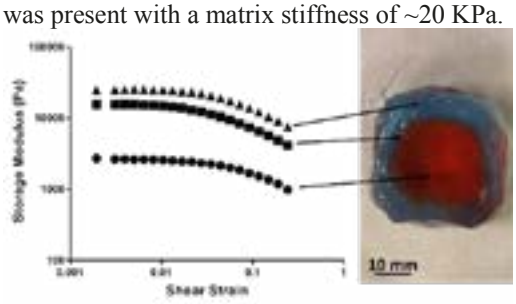

Fig. 1: Fabrication and rheological characterisation of a biphasic, gellan gum IVD analogue.

DISCUSSION & CONCLUSIONS: These data highlight the potential to utilise SLAM for the generation of constructs that can reflect the heterogeneous nature of the IVD. A single structure was successfully fabricated with matrix stiffness' that reflect the mechanical properties of the native tissue[4]. The printed constructs represent an acellular proof of concept for the use of suspended hydrogel printing in the generation of human IVD analogues. Incorporation of biological material such as cells and growth factors will be subsequently explored along with the inclusion of other biomaterials in order to better replicate the cellular and chemical structure of the IVD.

ACKNOWLEDGEMENTS: The authors acknowledge funding from the Wellcome Trust Institutional Strategic Support Fund to Advanced Materials in Medicine.

REFERENCES: [1] Baumgartner, L. *et. al.* (2021) Int. J. Mol. Sci. 22 (2), 703. [2] Van Uden, S. *et. al.* (2017) Biomater. Res. 21 (22). [3] Moxon, S.R. *et. al.* (2017) Adv. Mater. 29 (13), 1605594. [4] Kuo, Y.W. Wang, J.W. (2010) Spine. 35(16), E743-52. [5] Bron, J.L. *et. al.* (2011) J. Mech. Behav. Biomed. Mater. 4(7), 1196-1205

Functionalised Nanosurfaces for Animal-Product Free 3D-Substrates

M. T Shephard[1], T. P Dale[1], Y. Yang[1] and N. R Forsyth[1]

[1]*Guy Hilton Research Centre, School of Pharmacy and Bioengineering, Keele University, GB*

INTRODUCTION: Regenerative medicine approaches have established a substantial global market due to their potential as effective therapeutics for treating and curing diseases that remain refractory to routine pharmaceutical driven approaches and their emergence as an invaluable tool in the drug testing and discovery market. Intriguingly, the precise mechanisms of action remain open to debate due to the lack of reliable systems that enable robust interrogation while replicating *in vivo* complexity. For example, multiple cell type incorporation in a 3D environment, air-liquid interface (ALI) and simultaneous isolation of bioactive molecules those cells secrete. As such, new technologies and apparatus are urgently needed to keep pace with the demand for more controlled systems.

METHODS: Polycaprolactone (PCL) nanofiber membranes are electrospun to produce either highly aligned or randomly oriented membranes with controlled fiber diameter and thickness [1]. Nanofiber membranes are modified using our patent-filed functionalisation process which allows cell attachment without the need for biological molecule surface coating. Nanofiber membranes are mounted onto silicone rings when culturing PSCs or to the base of cell culture plate inserts to allow the generation of an ALI lung model.

RESULTS: Pluripotent stem cells (PSCs) do not attach to native PCL nanofiber membranes. Upon functionalisation, cell attachment, proliferation and colony formation are observed (Fig. 1A). These PSC colonies maintain pluripotency-associated markers for extended culture periods in xeno-free conditions whilst also staining negative for markers of differentiation (Fig. 1B).

Culture of porcine distal lung stem cells was achieved on nanofiber membranes mounted to the base of cell culture inserts. Differentiation to functional lung epithelial cells after 21 days in defined culture stained positive for both cilia and mucous production (Fig. 2A). An ALI was generated through the establishment of a tightly-packed monolayer producing TEER measurements (Fig. 2B).

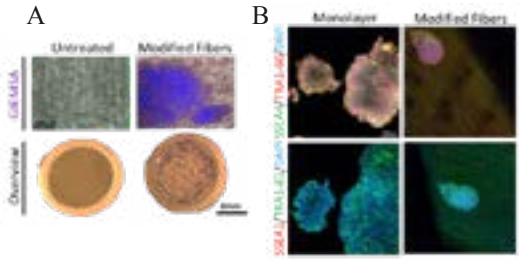

Fig. 1: (A) Functionalisation of nanofibers allows cell attachment and PSC colony formation. (B) Xeno-free maintenance of PSCs after 7 days of culture on nanofiber membranes stained for pluripotency-associated markers.

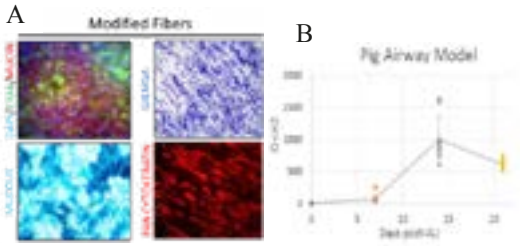

Fig. 2: (A) Differentiated lung cells cultured on nanofibers staining for cilia and mucous producing cells. (B) ALI TEER measurements.

DISCUSSION & CONCLUSIONS: We have created a unique system/apparatus that can be used for many different aspects of regenerative medicine development to culture cells in native 3D environments, is easily scalable, has a long shelf life and costs relatively little compared to current practice.

ACKNOWLEDGEMENTS: This template was modified with kind permission from eCM conferences Open Access online periodical & eCM annual conferences. This research was funded through MRC Confidence in Concept, Midlands Innovation Commercialisation of Research Accelerator and North Staffordshire Medical Institute grants.

REFERENCES: [1] Kumar D et al. Self-renewal of human embryonic stem cells on defined synthetic electrospun nanofibers. Biomed Mater. 2015 Nov 27;10(6):065017.

Dental Tissue Engineering Using Diabetic Bone Marrow Mesenchymal Stromal Cells

Nancy Hussein[1,2], Elena Jones[3], Josie Meade[1], Hemant Pandit[3], and Reem El-Gendy[1,4]

1 Division of Oral Biology, School of Dentistry, University of Leeds, UK

2 Department of Oral Medicine and Periodontology, Faculty of Dentistry, Mansoura University, Egypt

3 Leeds Institute of Rheumatic and Musculoskeletal Medicine, School of Medicine, University of Leeds, UK

4 Department of Oral Pathology, Faculty of Dentistry, Suez Canal University, Egypt

INTRODUCTION: Periodontal disease (PD) is an inflammatory disease that affects the tooth attachment apparatus and can lead to tooth loss. A bidirectional relationship between PD and diabetes has been established. Obesity is a common risk factor for both conditions and also for osteoarthritis (OA) with growing number of patients undergoing knee replacement surgery. The excised joints represent a readily available source of autologous stem cells sparing additional surgeries for cells harvesting. Characterization of bone marrow mesenchymal stromal cells (BM-MSCs) from osteoarthritic joints of diabetics is therefore fundamental for understanding the impact of diabetes on these cells and whether they can be used for periodontal tissue regeneration.

METHODS: BM-MSCs were isolated from osteoarthritic knee joints of type 2 diabetic and non-diabetic donors using collagenase digestion method. Cultured cells were compared for their proliferative capacities using colony forming unit (CFU) and population doubling time (PDT) assays. The osteogenic potentials of BM-MSCs were investigated under osteogenic conditions (OC) and their calcium deposits were compared using Alizarin Red staining and quantification and alkaline phosphatase staining after 1, 2 and 3 weeks in culture.

RESULTS: Diabetic BM-MSCs contained 16% fewer CFUs compared to non-diabetic cells at passages 1/2 and the median PDT of diabetic cells was 20% higher than that of non-diabetic BM-MSCs up to passage 5.

Diabetic BM-MSCs calcification at all time points under OC was on average 39% of that shown by non-diabetic cells. The intensity of alkaline phosphatase staining of both diabetic and non-diabetic cells was increased under OC vs basal conditions and by time in culture – both reflecting changes seen with Alizarin Red staining.

DISCUSSION & CONCLUSIONS: These preliminary results show that osteoarthritic BM-MSCs from type 2 diabetic patients have weaker proliferative and osteogenic capacities compared to osteoarthritic non diabetic cells. This work has future clinical implications for BM-MSCs based dental tissue engineering particularly for periodontal therapy under diabetic conditions.

ACKNOWLEDGEMENTS: NH would like to thank the Egyptian Ministry of Higher Education and the Egyptian Cultural and Educational Bureau in London for funding her PhD scholarship.

Tissue engineered cardiac patches for the treatment of post-MI heart failure using natural polymers and human iPSC-derived cells

ATR. Fricker[1], DA. Gregory[1], S. Harding[2], I. Roy[1,2]

[1]Department of Materials Science and Engineering, Faculty of Engineering, University of Sheffield, [2] National Heart and Lung Institute, Faculty of Medicine, Imperial College London

INTRODUCTION: Worldwide, cardiovascular diseases (CVDs) remain the leading cause of death, contributing a huge burden on healthcare providers. Myocardial infarction (MI) is one of the most fatal results of CVDs as it can lead to ultimate heart failure. Available treatments are used to mitigate many of the symptoms of MI, however they are not designed to repair the damaged tissue. A proposed solution to this is a regenerative treatment using a tissue engineered myocardial patch which would deliver healthy cells to repopulate the infarct area. In this research, natural and biocompatible materials, a polyhydroxyalkanoate (PHA)[1-3] and alginate[3], are used with the aim of producing a cellular multimaterial myocardial patch for this purpose. The patch would incorporate human induced pluripotent cardiomyocytes (hiPSC-CMs) and endothelial cells (hiPSC-ECs).

METHODS: Bacterial fermentation of *Pseudomonas* species was carried out to produce the PHA poly(3-hydroxyocatnoate-*co*-3-hydroxydecanoate), P(3HO-*co*-3HD), and this was purified and extracted from the bacteria using Soxhlet extraction. Resazurin assays with the C2C12 myoblast cell line were used to test the biocompatibility of P(3HO-*co*-3HD) and alginate hydrogel, the polymers were 3D printed (fused deposition modelling) to produce a multimaterial patch, with C2C12 cells encapsulated in the alginate and 3D-bioprinted. hiPSC-CMs and hiPSC-ECs were produced from (hiPSCs), seeded onto P(3HO-*co*-3HD) films, live/dead stained, and functionally analysed.

RESULTS: P(3HO-*co*-3HD) has been successfully produced and characterised to confirm its chemical structure and 3HO:3HD molar ratio; mechanical properties showed that it was highly elastomeric, making it a suitable polymer for myocardial applications; and thermal properties, including a melting point of around 54°C making it easy to 3D print. P(3HO-*co*-3HD) and alginate were shown to both be non-cytotoxic via the resazurin assay. 3D printing was carried out with these materials, with C2C12 cells encapsulated in the alginate (Fig. 1). High resolution, cellular multimaterial patches were successfully produced, while maintaining cell viability. To improve the cell types included in the patch, hiPSC-CMs and hiPSC-ECs were produced, with initial results showing that they adhere to P(3HO-*co*-3HD) with good viability, and retain functionality through beating and calcium handling, as seen with Fluo-4 imaging.

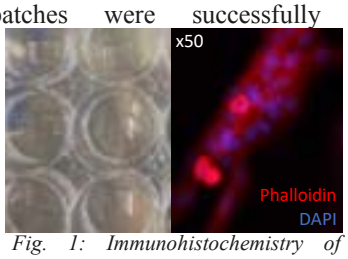

Fig. 1: Immunohistochemistry of C2C12 cells encapsulated in alginate and 3D printed

DISCUSSION & CONCLUSIONS: Multimaterial patch production and successful encapsulation and printing of cells shows promise for the development of a functional cellular multimaterial patch. Future aims in this project are to include hiPSC-ECs and hiPSC-CMs in the multimaterial patch before carrying out *in vitro* and *in vivo* experiments in a rodent MI model.

ACKNOWLEDGEMENTS: We thank the University of Sheffield for ATR Fricker's PhD scholarship.

REFERENCES:

[1]Majid QA, *et al*. Natural biomaterials for cardiac tissue engineering: a highly biocompatible solution. Frontiers in Cardiovascular Medicine 7, 192, 2020

[2]Bagdadi AV, *et al*. Poly(3-hydroxyoctanoate), a promising new material for cardiac tissue engineering. Journal of Tissue Engineering and Regenerative Medicine 12, 495, 2018

[3]Rai R, *et al*. Medium chain length polyhydroxyalkanoates, promising new biomedical materials for the future. Materials Science and Engineering: R: Reports 72, 29, 2011

Identifying and characterizing the phenotype of cells for use in peripheral nerve tissue engineering

Jenny Katsouli[1], Owein Guillemot-Legris[2], James B Phillips[2], Rebecca Powell[2]

[1] *UCL Division of Medicine, Royal Free Campus, Rowland Hill Street, London, NW3 2PF, UK.*
[2] *UCL Centre for Nerve Engineering, University College London, London WC1E 6BT, UK*

INTRODUCTION: Repair Schwann cells have a central role in regeneration following peripheral nerve injury - secreting neurotrophic factors, forming Bands of Büngner, stimulating vascularisation, and interacting with macrophages. A Target Phenotype Profile (TPP), (Table.1) was determined through a literature review. This gene panel can help assess in vitro the therapeutic potential of cellular options, intended for nerve tissue engineering. This study aimed to utilize the TPP to appraise the peripheral nerve regenerative potential of Schwann cell precursors (SCPs), which are derived from human induced Pluripotent Stem Cells (hiPSCs).

METHODS: Initially, a literature review was conducted to construct the TPP, based on gene expression patterns associated with repair phenotype Schwann cells (Table 1) [1,2]. The relative expression of these markers was then measured using RT-qPCR, as hiPSCs differentiated towards SCPs. The ability of the SCP secretome to accelerate neuronal growth in vitro was tested using rat dorsal root ganglia (DRG) neurites cultured in SCP conditioned medium.

Table 1. Target phenotype profile for therapeutic cells. Includes the most critical markers which are upregulated to achieve a phenotype associated with the repair process in Schwann cells. In bold are those genes associated with multiple phenotypes.

Phenotype	*Upregulated Markers*
Immune cell interaction	**LIF**, IL1A, TNF-α, IL1β, MCP-1
Nerve bridge formation	**NRG1**, **SOX2**, **cJUN**, **EPO**, ROBO1, NCAM, NCAD
De-myelination	**SOX2**, **NRG1**, ID4, PAX3, NOTCH-1, ID2, OCT6, PMP22, PRX
Proliferation	**SOX2**, **cJUN**, **EPO**
Axonal Elongation	**LIF**, **EPO**, **cJUN**, VEGFA, ARTN, BDNF, NTF3, NCAD, p75NTR, PTN, FLT1, GDNF, IL6, NGF
Remyelination	**EPO**, ITGB1, DAG1
Repair phenotype maintenance	**cJUN**, STAT3
Autophagy	AXL, MERTK, ATG7

RESULTS: There was an upregulation of several markers associated with the repair phenotype during the differentiation of SCPs, (Table 2). SCPs displayed relative increases in gene expression of membrane proteins NCAD and NCAM1 and secreted factors EPO, GDNF and VEGFA, compared to hiPSCs (Table.2). DRG neurite outgrowth assay was increased in the presence of the SCP conditioned medium (Fig.1).

DISCUSSION & CONCLUSIONS: SCPs derived from hiPSCs display regeneration-associated markers in vitro and promote neurite growth, indicating they could be good candidates for nerve tissue engineering.

Table 2. Changes in TPP marker expression as hiPSCS differentiate towards SCPs (+: increase, -: decrease)

Gene	**cJUN**	**SOX2**	**NCAD**	**NCAM1**	**ROBO1**	**VEGFA**	**EPO**	**GDNF**
Expression	+	-	+	+	-	+	+	+

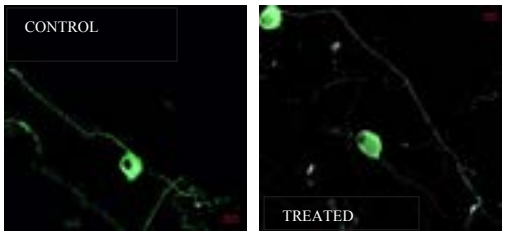

Fig.1: Immunofluorescent staining of DRG neurites. SCP conditioned medium treatment boosts axonal growth following 3 days of incubation. Scale bar 20μm.

REFERENCES: 1. Jessen, K.R. and Mirsky, R. (2019). The Success and Failure of the Schwann Cell Response to Nerve Injury. Frontiers in Cellular Neuroscience, [online] 13. Available at: https://www.ncbi.nlm.nih.gov/pmc/articles/PMC6378273/ **2.** Nocera, G. and Jacob, C. (2020). Mechanisms of Schwann cell plasticity involved in peripheral nerve repair after injury. Cellular and Molecular Life Sciences, 77(20), pp.3977–3989.

AKNOWLEDGMENTS: We would like to thank the Medical Research Council (MRC) for the financial support. Grant No. MR/N013867/1

Investigating how secreted factors from adipose tissue alter myofibroblast and scar phenotype

S.J. Higginbotham[1], V.L. Workman[1], N.H. Green[1], V. Giblin[2], D.W. Lambert[3], V. Hearnden[1]
[1] Department of Materials Science and Engineering, The University of Sheffield, Sheffield S3 7HQ, UK [2] Sheffield Teaching Hospitals NHS Trust, Sheffield, S10 2JF, UK [3] School of Clinical Dentistry, The University of Sheffield, Sheffield, S10 2TA, UK

INTRODUCTION: Hypertrophic dermal scarring occurs as a result of aberrant activation of fibroblasts to myofibroblasts during wound healing by the action of transforming growth factor β-1 (TGFβ-1) and other factors. This leads to excessive production of extracellular matrix components such as collagen and fibronectin, causing the formation of thick, painful scar tissue which limits mobility and lowers quality of life (1). Autologous fat grafting has been shown to promote tissue regeneration and lower the characteristic thickness of these scars. However, the mechanisms behind this effect are yet to be fully characterized and represents a gap between the literature and clinical practice (2). This work further examines the mechanisms behind which types of adipose tissue can regenerate and reverse scars, specifically its role in fibroblast to myofibroblast differentiation.

METHODS: Using lipoaspirate from NHS patients (NHS ethics 15/YH/1077), adipose tissue was processed in line with current clinical practices (3). Paracrine factors from the adipose tissue were collected by conditioning in cell culture medium for 72 hours. This medium was then added to human dermal fibroblasts alongside TGFβ-1 (which promotes myofibroblast differentiation in vitro). Following this, RNA and protein expression was examined to test if adipose tissue paracrine factors could inhibit myofibroblast differentiation. Finally, the ability of adipose tissue conditioned medium to increase proliferation of fibroblasts treated with TGFβ-1 was assessed using a Ki-67 staining method.

RESULTS: Analysis of the expression of myofibroblast marker α-SMA indicated that myofibroblasts differentiation was inhibited by adipose tissue conditioned medium (Fig. 1). Additionally, fibroblast proliferation was significantly increased when treated with TGFβ-1 and adipose tissue conditioned medium.

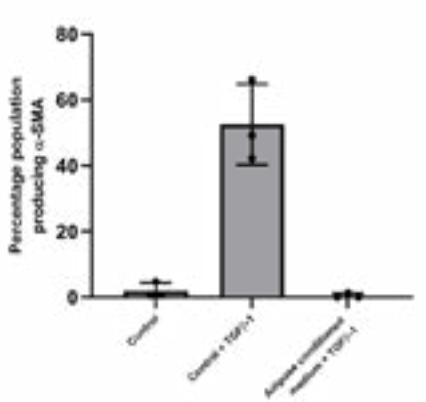

Fig. 1: The percentage of cells producing α-SMA protein following the addition of TGFβ-1 and adipose conditioned medium.

DISCUSSION & CONCLUSIONS: Our data demonstrated that factors secreted from adipose tissue are capable of increasing cellular proliferation and inhibiting canonical TGFβ-1 signalling in a scar environment. Taken together, this presents a potential mechanism responsible for adipose tissue's regenerative abilities post scarring, by reducing scar production while increasing cellular proliferation. This presents a possible pathway for tailoring future treatments and is a step towards further understanding the role and potential of adipose tissue for scar regeneration and wound healing.

ACKNOWLEDGEMENTS: The authors would like to acknowledge ESPRC, the Sheffield Hospital Directorate of Plastic, Reconstructive Hand and Burns Surgery and the Wolfson Light Microscopy facility.

REFERENCES:

1. Darby I. et al. Clin Cosmet Investig Dermatology 2014; 4 (7) 301-311
2. Klinger M. et al. Plast Reconstr Surg 2007; 119 (5) 1409-1422
3. Tonnard P. et al. Plast Reconstr Surg 2013; 132 1017-1026

A bioengineered bone marrow niche model to support long-term HSCs *in vitro*

H. Donnelly[1], E. Ross[2], C. West[3], B. Peault[3], M. Salmeron-Sanchez[1], M. J. Dalby[1]

[1]Centre for the Cellular Microenvironment, University of Glasgow, UK, [2] Aston University, Birmingham, UK, [3]MRC Centre for Regenerative Medicine, University of Edinburgh, UK

INTRODUCTION: Hematopoietic stem cells (HSCs) have the ability to regenerate the entire blood and immune system[1], as such, they hold enormous clinical potential. In vivo they are supported by mesenchymal stromal cells (MSCs) and pericytes in a specialised microenvironment that provides physical and functional regulatory cues, termed the bone marrow (BM) niche. Once HSCs are removed from the niche their ability to self-renew is lost quickly, cells rapidly proliferate and spontaneously differentiate away from the long-term reconstituting (LT-HSC) phenotype in a matter of days rendering them clinically ineffective[1]. Here, we have developed a system to recapitulate properties of the BM niche microenvironment to retain niche phenotypes in a stromal cell population, which in turn, support an LT-HSC population *in vitro*.

METHODS: Using poly (ethyl acylate) (PEA) to promote material-driven unfolding of the extracellular matrix protein fibronectin (FN), we tether BM niche associated growth factors (GF) (e.g. BMP-2) to the exposed GF binding domain on FN[2]. A collagen type I hydrogel in the stiffness range of the bone marrow (~0.1 kPa)[3] is then incorporated.

Phenotypic analysis of stromal stem cells is carried out by NGS, flow cytometry and fluorescent microscopy. Analysis of HSCs is carried out using flow cytometry and functional assays, such as long term culture-initiating cell (LTC-IC) and colony forming unit (CFU) assays.

Metabolomic analysis and siRNA techniques are used to identify metabolic regulations associated with the BM niche phenotype.

RESULTS: We demonstrate the introduction of a collagen hydrogel (+gel) in the stiffness range of the BM leads to long-term maintenance of a niche phenotype in a stromal stem cell population. Gel addition leads to significantly increased expression of nestin (Fig 1), a key niche stromal marker[4], production of HSC maintenance cytokines CXCL12 and SCF, and changes to metabolic regulation. Upon co-culture with HSCs, we found that this niche-like system is able to support HSCs in culture, yetthe most desirable LT-HSC population is most effectively maintained in +gel conditions.

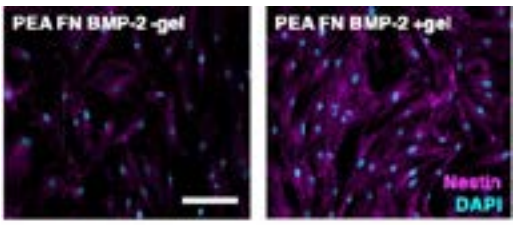

Fig. 1: Hydrogels in stiffness range of BM increase nestin expression in stromal stem cells: -gel (left) vs. +gel (right). Scale bar is 100 µm.

DISCUSSION & CONCLUSIONS: This material-based system offers a platform for investigation into fundamental mechanisms of stem cell regulation, such as maintenance of stemness and metabolic processes. Platforms such as these can be further developed for use as a non-animal technologies, providing more humanised models for genotoxicity screening of drugs, small molecules and cellular therapies.

ACKNOWLEDGEMENTS: We gratefully acknowledge support of EPSRC grant EP/P001114/1 and C.A. Smith for technical support.

REFERENCES:

1. Jagannathan-Bogdan, M. & Zon, L. I. Development 140, 2013.

2. Cheng, Z. A. et al. Advanced Science. 1800361, 2018.

3. Jansen, L. A. et al. Journal of the Mechanical Behavior of Biomedical Materials. 50, 2015.

4. Méndez-Ferrer, S. et al. Nature 466, 2010.

Human Cartilage Developmental Model Using Embryonic Stem Cells Cultured Within 3D Hydrogels

Miguel J.S. Ferreira[1], Michael Buckley[2], Susan J. Kimber[3], Marco A.N. Domingos[1]

[1]Department of Mechanical, Aerospace and Civil Engineering, Faculty of Science and Engineering & Henry Royce Institute, The University of Manchester, [2]Manchester Institute of Biotechnology, The University of Manchester, [3]Division of Cell Matrix Biology and Regenerative Medicine, Faculty of Biology, Medicine and Health, The University of Manchester.

INTRODUCTION: During development, articular cartilage (AC) is generated from the lateral plate mesoderm, an embryonic structure that gives rise to the limb bud and later forms the appendicular skeleton. Strategies to recapitulate cartilage development using human embryonic stem cells (hESCs) have been established [1-4]. However, current methods are complex and expensive [1-3], offer reduced control over the expression of key developmental markers [4], and lack translation into 3D culture using cell-laden hydrogel systems [1-4], a critical step towards applications in AC tissue engineering. In order to address these limitations, this work is aimed towards the establishment of a simple and cost-efficient strategy to guide hESC differentiation through the developmental route towards the generation of chondroprogenitor cells, and use them to generate a model of limb bud chondrogenesis in 3D.

METHODS: hESC line Man13 (5) was differentiated using a multi-step protocol with time-dependent modulation of WNT signalling using CHIR (WNT activator) and C59 (WNT inhibitor) and activation of retinoic acid (RA) signalling using TTNPB for 9 days. Then, hESC-derived chondroprogenitor cells were allowed to form aggregates for 72h. Finally, cell aggregates were encapsulated in alginate or alginate/type-I collagen hydrogels and cultured for a further 14 days in DMEM supplemented with ascorbate-2-phosphate, proline, ITS, dexamethasone, and L-glutamine. Cell viability was evaluated using live/dead staining and cell phenotype was characterised over the course of differentiation by qRT-PCR and stained using Alcian Blue and Safranin O.

RESULTS: Treatment of hESCs with CHIR for 48h followed by C59 under RA activation led to the acquisition of a lateral plate mesoderm-like phenotype with increased expression of markers FOXF1, HAND1, HAND2 on days 3-4. Then, the application of a second pulse of CHIR resulted in the controlled expression of limb bud mesoderm marker PRRX1 and forelimb marker TBX4 on day 6. Further treatment with TTNPB led to the acquisition of a chondrogenic phenotype on day 9, with upregulation of key transcription factors SOX5 and SOX9, and cartilage extracellular matrix components COL2A1 and ACAN. Culture of aggregates from day 9 in 3D alginate-based hydrogels resulted in high levels of cell viability, maintained expression of chondrogenic makers for up to a further 14 days, and positive staining for sulfated glycosaminoglycans and proteoglycans.

DISCUSSION & CONCLUSIONS: These findings suggest that the modulation of WNT and RA signalling alone may be sufficient to guide hESCs towards lateral plate mesoderm and limb bud-like stages prior to chondrogenesis, in a simple and cost-efficient manner. The use of alginate-based hydrogels may serve as a suitable platform to translate differentiation from 2D into a 3D culture system towards the development of a new AC tissue engineering strategy for regenerative medicine and *in vitro* tissue modelling applications.

ACKNOWLEDGEMENTS: This work was supported by the Henry Royce Institute for Advanced Materials, with financial support from the EPSRC/MRC CDT in Regenerative Medicine (EP/L014904/1).

REFERENCES: 1. Oldershaw et al., Nat. Biotechnol. 28:1187–1194, 2010. 2. Wang et al., Stem Cell Res. 39:101497, 2019. 3. Loh et al., Cell. 166: 451–468, 2016. 4. Kawata et al., Stem Cell Reports. 13: 530–544, 2019. 5. Ye et al., Stem Cell Res Ther. 8:128, 2017.

Single step, centrifugation-free cell washing and medium exchange for cellular therapeutics

T Carvell[1], MM Zadeh[2], JDM Campbell[3], L Milne[3], AR Fraser[3] and H Bridle[1]

[1] Heriot-Watt University, Edinburgh, GB, [2] Food Water Waste Group, University of Nottingham, GB, [3] Scottish National Blood Transfusion Service, Edinburgh, GB.

INTRODUCTION: Cellular therapies are part of a rapidly expanding area of medicine used to meet a wide range of unmet needs including the treatment of cancer and metabolic diseases but also in regenerative medicine. The manufacturing of cellular therapies remains challenging and time intensive often requiring multiple centrifugation stages that can result in cellular damage and poor cell recovery. Here, we describe a centrifugation-free media exchange and cell processing microfluidic device.

METHODS: For the experiments described 2-loop spiral-shaped microfluidic devices were manufactured (Epigem Ltd, GB), Figure 1. Initially the devices were comprised of 2 inlets (inner: 320µm, outer: 160µm in width) and 2 outlets (inner: 160µm, outer: 320µm in width) with a microchannel between the two (H: 80µm, W: 480µm) with 13.8mm spacing between the loops of the spiral. A new design retained the same microchannel geometry but with identical dimensions for the 2 inlets (W: 240µm) and 4 outlets (W:120µm), respectively.

Characterisation of devices was performed by injecting polystyrene beads of biologically relevant size (Sigma-Aldrich, UK) at various flow rates into the wide inlet using a syringe-pump (Fusion 100, Chemyx Inc., USA and neMESYS 1000N, Cetoni GmbH, Germany) alongside PBS at the narrow inlet. High-speed imaging utilising an inverted fluorescence microscope (TC-100, Medline scientific) equipped with a 10-bit CCD camera (Mako U-130B, Allied Vision Technologies) was employed to capture particle, and later, cell positions near to the outlets. Human monocytic cell line THP-1 was used to investigate separation of functional cells and assessed by cell culture pre- and post-device processing. Cells were injected into the wider inlet and DMEM/FCS medium was injected at the narrow inlet to assess the device capacity for cell recovery, media exchange properties and post-processing cell viability.
RESULTS: Experiments using the original device demonstrated that medium exchange efficiency was highest at 800µl/min, determined to be 82%. Increasing the flow rate to 1ml/min, i.e. higher throughput, resulted in a reduction in cell recovery (80%) but with similar media exchange efficiency (within 1%) observed at 800µl/min. As a measurement of impact of microfluidic processing on the cells, the number, and viability, of cells, after 96 hours of culturing was determined. Cell counts were 1.74-2.34x10^6 cells/mL across the 500µl/min-1ml/min range tested compared to 2.3x10^6 cells/ml in the control sample, while cell viabilities in all samples were >95%.

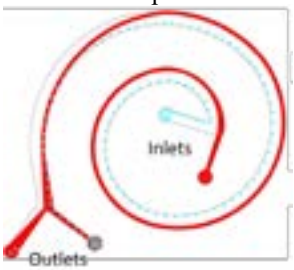

Figure 1 – Schematic depicting original spiral microfluidic device and use for medium (red) exchange and cell (blue) concentrating applications.

Preliminary data obtained using the 4-outlet device, investigating higher throughput, suggests a separation efficiency of 10µm particles of >98% at 15mL/min. Further experiments using cellular material are required.

DISCUSSION & CONCLUSIONS: The device exploits both the inertial forces and the secondary counter-rotating Dean vortices generated by the architecture of the spiral microchannel to efficiently focus particles and cells towards specific outlets whilst exchanging them to a fresh medium. The two-outlet device focused particles and cells towards the inner wall of the spiral whereas at higher flow rates above 15mL/min, the new device is highly efficient at focusing particles toward the outer wall of the spiral enabling a high recovery rate of cells to potentially revolutionize cell therapy manufacturing processes.

Role of Scaffold Geometry in Tympanic Membrane Tissue Engineering

S. Anand[1], T. Stoppe[2], M. Neudert[2], S. Danti[3], L. Moroni[1], C. Mota[1]

[1]MERLN Institute for Technology-Inspired Regenerative Medicine, Maastricht University, Maastricht, NL, [2]Technische Universität Dresden, Carl Gustav Carus Faculty of Medicine, Dresden, DE, [3]Department of Civil and Industrial Engineering, University of Pisa, Pisa, IT

INTRODUCTION: The human tympanic membrane (TM) is a thin, concave structure of the middle ear that captures sound waves from the environment and transforms them into mechanical motion. Successful transmission of these acoustic vibrations to the inner ear is attributed to its precise three-dimensional (3D) design comprising of radial and circumferential collagen fibers [1, 2]. This work presents a combination of theoretical and experimental approaches toward understanding the role of these geometrical features in creating biomimetic eardrum scaffolds.

METHODS: A Python script was developed for modelling the anatomical architecture of the human TM. Theoretical comparisons were performed on COMSOL Multiphysics by simulating the appropriate mechanical and acoustical interaction of the selected cases. A dual scale fabrication strategy combining electrospinning and additive manufacturing was implemented for creating hierarchical TM scaffolds *(Fig. 1A)*. The mechano-acoustical response of the fabricated constructs was evaluated by applying the techniques of macroscopic indentation and laser Doppler vibrometry (LDV). Finally, human dermal fibroblasts (hDFs) and human mesenchymal stromal cells (hMSCs) were cultured to assess the influence of 3D hierarchy on cellular alignment and subsequent collagen deposition.

RESULTS: The Python script served as a versatile and robust tool for generating TM models with diverse anatomical features. *In silico* investigation of the chosen designs suggested a geometrical dependency of their mechanical and acoustical responses *(Fig. 1B)*. The macro-indentation results corroborated the findings of the theoretical simulations, and radially aligned scaffolds were noted to show a Young's modulus closer to that of the human eardrum *(Fig. 1C)*. In addition, the LDV measurements demonstrated all the fabricated constructs to be acoustically comparable to the native tissue. The biological studies performed with hDFs and hMSCs, revealed a favorable influence of 3D hierarchy on cellular alignment and subsequent deposition of the extracellular collagen matrix *(Fig. 1D)*.

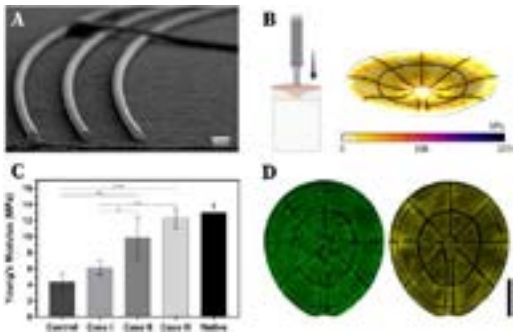

Fig. 1: (A) Demonstration of hierarchical TM scaffolds. (B) Computational simulation of the macro-indentation study. (C) Comparative Young's moduli for the chosen geometrical cases. (D) F-actin filaments of the cultured cells at day 7 (left); extracellular collagen deposited at day 14 (right). Scale bar = 3 cm.

DISCUSSION & CONCLUSIONS: In this study, we investigated the relevance of scaffold geometry in TM tissue engineering by performing mechanical, acoustical and biological characterizations. The optimized biofabrication strategy allowed the creation of biomimetic constructs within the dimensions of native eardrum. In general, the presence of radially aligned fibers was observed to have a more prominent effect as compared to their circumferential counterparts. Furthermore, a higher cellular orientation and collagen production was obtained in regions along the additive manufactured fibers.

ACKNOWLEDGEMENTS: This work is a part of the *4NanoEARDRM* project, receiving funding from EuroNanoMed III, the ERA-NET Cofund Action on Nanomedicine under Horizon 2020.

REFERENCES:

[1] Mota, C. et al. *Biofab*. 2015; 7(2):025005.
[2] Anand, S. et al. *Adv. Healthc. Mater*. 2021; 2002082.

Cellular response to substrate topography, chemistry and cyclical loading

V. Alageswaran[1], R. L. Dimmock[1], V. George[1], Y. Yang[1]

[1] *School of Pharmacy and Bioengineering, Keele University, Stoke-on-Trent, UK*

INTRODUCTION: Biomaterials have been used as substrates to dictate cellular response, by influencing cell proliferation as well as cellular phenotype. Here, we are using biocompatible substrates with modified micro, nano-topographies including wrinkled surfaces, ligand modified films and nanofibers to study cellular response. We hypothesize that substrates' topography with different dimensions and their chemistry determine the key ligand protein adsorption on the substrates, which affect cells' aggregation status, colony formation and capacity to tolerate mechanical stimulation. This study used two substrate materials, polylactic acid (PLA) and polydimethylsiloxane (PDMS), inducing topographies at micro- and nanometer scale, to examine immortalized Human Embryonic Kidney 293 (HEK293) cells' adherence to materials and cell integrity post-stimulation. This allowed us to gauge the topographical cues that facilitate cell re-adhesion after stretch on the various substrates. Through the use of a live-cell imager, we were able to monitor whether the various substrates directly affect the colony morphologies through contact guidance and whether the cyclical loading on various substrates influences the reattachment of cells.

METHODS: HEK293 cells in passage 48 were used. The cell seeding density was kept at 40k per sample. PLA nanofibers were manufactured in both aligned and random orientation through electrospinning. The nanofiber diameter was ranged 500-700 nm. 5% curing agent PDMS was cast at 85°C. Wrinkling was generated by exposure of pre-strained substrate to strong acids or low temperature oxygen plasma in vacuum. Following the cell attachment and culture of HEK293 cells on the various substrates for 2 days, the substrates underwent cyclical load by a novel magnetic ball indentation bioreactor which stretched the substrates for 30 minutes at 1 Hz. After 24 hours post-culture, the samples were fixed and morphology was examined for differences in their cytoskeletal organization and attachment.

RESULTS: HEK293 cells formed flat clusters on PLA and PDMS films, whilst HEK293 cells formed more 3D-like clusters in PLA nanofiber meshes with aligned cluster in aligned fiber and irregular shape cluster in randomly aligned nanofiber. Micro-meter scale wrinkled PDMS substrates did not trigger 3D-like clusters. Cell reattachment was evident on all substrates after 24 hour post stimulation. The tissue culture plastic (TCP) control and random aligned nanofibers showed different colony morphology and phalloidin expression. Aligned nanofibers not only produced greatest topography-matched cell alignment, but also increased cell proliferation post-stimulation. This was not replicated in PDMS or PLA films post-stimulation. Furthermore, aligned nanofibers were able to distribute the cyclical load evenly with directionality, in contrast to random nanofibers.

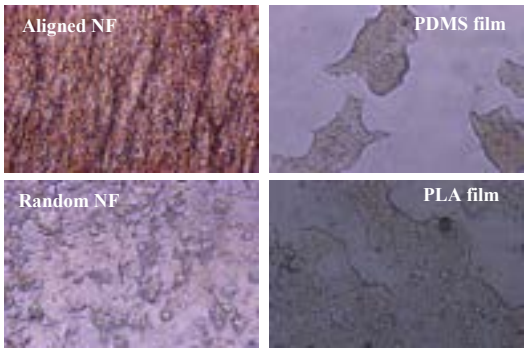

Fig. 1: The cell morphology on various substrates after 2-day static culture

DISCUSSION & CONCLUSIONS: Nanofibers (aligned or random) were able to produce HEK cell colonies that acquired 3D formations which outperformed 2D films or wrinkled surfaces in proliferation and cytoskeletal dynamics. This supports niche-dependent effects through improved contact guidance. Aligned nanofibers further enhanced reattachment and improved proliferation post-stimulation suggesting the type of topography which stimulus is applied on can positively influence cell behavior.

Investigation of the Volatilome of Stem Cells using Selected Ion Flow Tube Mass Spectrometry

S. Barreto[1], NR. Forsyth[1], AV. Rutter[1]

[1]*Institute for Science and Technology in Medicine, School of Pharmacy and Bioengineering, Keele University, England, GB*

INTRODUCTION: Human pluripotent stem cells (hPSCs), such as embryonic stem cells (hESCs) and induced pluripotent stem cells (hiPSCs), have gathered tremendous attention as they have multiple applications in regenerative medicine. Therefore, it is not surprising that their cellular mechanisms, including metabolism, are being intensely studied. However, cellular metabolomics is challenging since cells' metabolomes are incredibly complex, composed of many different metabolites (e.g., lipids, peptides, organic acids, thiols, and carbohydrates) [1]. Measuring such great diversity relies on large-scale qualitative and quantitative analytical platforms, like mass spectrometry, which are often destructive (i.e., involve destructive metabolite extraction) and need complicated sample preparation procedures that, in turn, prevent real-time analysis of samples [1,2].
Furthermore, most of the current knowledge regarding hPSC metabolism results from assumptions based on cancer studies [3]. As a result, more research focusing specifically on the metabolism of hPSCs is needed to provide more tangible data on how metabolism and metabolites influence cellular processes responsible for establishing and maintaining stem cell self-renewal, pluripotency, and differentiation.
Analysing the volatile metabolites released by stem cells could give invaluable information regarding their metabolic processes. A strategy to efficiently detect such volatiles from cell samples is the use of selected ion flow tube-mass spectrometry (SIFT-MS). SIFT-MS allows for accurate analyses of humid gaseous samples for several compounds simultaneously in real-time, without the need for sample preparation and collection that can compromise the sample [2].
This study aims to identify a Volatile Organic Compound (VOC) profile of hPSCs using SIFT-MS.

METHODS: Media samples from two hESC lines (SHEF-1 and -2) and one hiPSC line (ZK2012L), cultured in xeno-free conditions and 2% or 21% oxygen, will be transferred into glass bottles for SIFT-MS measurements. The headspace of the bottles will be purged with dry and sterile air (20% oxygen and 80% nitrogen mixture) to strengthen the quality and reproducibility of the VOC data produced. The bottles will then be incubated for 16 hours at 37°C to accumulate VOCs before performing the measurements. Following this incubation, the gaseous headspace above the cells will be measured and analysed using SIF-MS.

RESULTS: We will utilise a kinetic library (a list of compounds and their known mass-to-charge ratios) to investigate differences of 10 expected VOCs (acetone, acetaldehyde, ethanol, butanol, pentanol, DMS/ethanethiol, hexanal, butyric acid, pentene, putrescine), which have been identified in a previous study [4], in the headspace of the stem cells cultured in the different conditions.

DISCUSSION & CONCLUSIONS: SIFT-MS could be employed as an additional non-invasive technique to identify and characterise stem cells in culture. Furthermore, we hope that this study will contribute to the establishment of a VOC blueprint for pluripotency and self-renewal, which, in turn, will enhance the understanding of metabolome dynamics of stem cells.

ACKNOWLEDGEMENTS: We would like to thank the EPSRC Doctoral Training Centre in Regenerative Medicine for funding this research (grant number EP/L015072/1).

REFERENCES: [1] Dunn WB, et al. (2005) *Analyst* **130**(5):606-625. [2] Rutter AV, et al. (2013) *Analyst* **138**(1):91-95. [3] Zhang J, et al. (2012) *Cell stem cell* **11**(5):589-595. [4] Al-Zubaidi MA (2018) Doctoral dissertation, Keele University

Kidney Tissue Engineering using Polyhydroxyalkanoates

S.M.D. Syed Mohamed[1], G. Welsh[2], I. Roy[1]

[1]Department of Materials Science and Engineering, Faculty of Engineering, University of Sheffield, UK, [2] Bristol Renal, Translational Health Sciences, Bristol Medical School, University of Bristol, UK

INTRODUCTION: End-stage kidney patients need to undergo haemodialysis and kidney transplantation due to renal failure. However, haemodialysis is never sufficient to reinstate normal kidney functions, especially in the glomerulus. A new tissue engineering approach utilises a bacterial polymer, polyhydroxyalkanoates (PHA) to develop a bioartificial kidney. PHA is a green polymer that is biodegradable, biocompatible, and bioresorbable.[1] There are two types of PHAs, short chain-length PHAs (scl-PHAs) that are normally stiff and medium chain-length PHAs (mcl-PHAs) that are elastomeric in nature. In this work we will use a PHA based scaffold to engineer a bioartificial filtration barrier to filter toxic waste in blood.

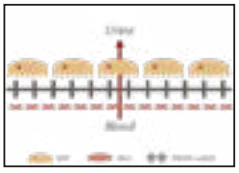

Fig. 1: Bioartificial filtration barrier utilising CIHP and GEnC, with P(3HO-co-3HD) as scaffold.

METHODS: Bacterial fermentation was carried out using a selected bacterial strain, fed by specific fatty acids to produce an mcl-PHA, P(3HO-*co*-3HD). This polymer will be subjected to 3D printing (Fused Deposition Modelling) to engineer a kidney bioartificial filtration barrier in the future (Fig. 1). The polymer produced was thoroughly characterised using; Gas Chromatography (GC) for monomer composition, Gel Permeation Chromatography (GPC) for polymer molecular weight, and Thermal Gravimetric Analysis (TGA) and Differential Scanning Calorimetry (DSC), both for thermal properties. Two types of glomerular cells, the conditionally immortalised human podocytes (CIHP) and the glomerular endothelial cells (GEnC) will be used.[2] CIHP was cultured onto the P(3HO-*co*-3HD) within 24-well plates and subjected to resazurin assay as a cytocompatibility test.

RESULTS: P(3HO-*co*-3HD) was produced with a yield of 40 g of polymer per 100 g of dry cell weight (40% dcw). The monomer composition of the polymer revealed a higher percentage of HO as compared to the HD. From the GPC, the average molecular weight, M_w was around 100,000 g/mol. Tensile testing confirmed the elastomeric nature of the polymer and a low melting temperature (T_m) enhanced the printability of the polymer. Cytocompatibility test showed for the first time that P(3HO-*co*-3HD) was highly compatible with glomerular cells, even more so than tissue culture plastic (TCP) (Fig. 2).

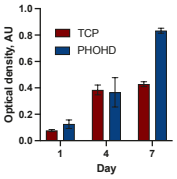

Fig. 2: Cytocompatibility result for CIHP on TCP and P(3HO-co-3HD).

DISCUSSION & CONCLUSIONS: This work aims to bio-mimic the glomerular functionality to ultimately develop a bioartificial kidney using a tissue engineering strategy. We therefore successfully produced and characterised a suitable biomaterial for this application. In addition, we conclusively showed that the polymer supported the adherence and growth of one of the podocytes. In future, the bioartificial filtration barrier developed using the combination of the P(3HO-*co*-3HD) along with two cell types will restore the ability of the glomerulus to filter toxin and waste in blood. This strategy will eventually lead to the development of a future wearable kidney.

ACKNOWLEDGEMENTS: S.M.D. Syed Mohamed is funded by the Government of Malaysia under Malaysia Department of Public Services.

REFERENCES: [1]Constantinides, C., et al., *In Vivo Tracking and 1H/19F MRI of Biodegradable Polyhydroxyalkanoate/Polycaprolactone Blend Scaffolds Seeded with Labeled Cardiac Stem Cells*. ACS Applied Materials Interfaces, 2018. 10(30): p. 25056-25068. [2]Kitching, A.R. and H.L. Hutton, *The Players: Cells Involved in Glomerular Disease.* Clinical Journal of the American Society of Nephrology, 2016. 11(9): p. 1664-1674.

Contractility signatures of cancer cells using 3D *in vitro* models

A. Micalet[1,2], J. Pape[2], Y. Javanmardi[1], S. Lasli[1], E. Moeendarbary[1*], U. Cheema[2*]
Presenting Author: Auxtine Micalet, auxtine.micalet.19@ucl.ac.uk
[1]*Departement of Mechanical Engineering, University College London (UCL)*
[2]*Division of Surgery and Interventional Sciences, University College London (UCL)*
**Joint senior authorship*

INTRODUCTION: The bio-mechanical characteristics of cancer cells and how these parameters affect tumorigenesis is now well recognised. In this study we aim to use 3D *in vitro* methods to assess the contractility signatures of various epithelial cancer cell-lines.

METHODS:

Contraction assays. 3D collagen type I hydrogels were set in a 24 well plate, with cancer cells mixed within the gel at densities of 500 k/mL, 1 M/mL and 2 M/mL. HT-29, HCT116, MDA-MB-231 and HDF cell-lines were used. HDF serve as a positive control as they are known to contract collagen hydrogels. After setting the hydrogels at 37°C for 15 minutes, the gels were detached from the well so that they were free floating. Contraction was observed over 96 hours.

Traction force microscopy (TFM). Soft (1 kPa) polyacrylamide (PA) gels were cast on glass bottom petri dishes. The gels contain 0.3 µL/mL of 0.1 µm red fluorescent beads. The glass surface was pre-treated with APTES and glutaraldehyde to allow the gel to adhere to the glass. The gels were functionalised using collagen type I to allow the cells to form integrin bonds with the gel surface. HT-29, HCT 116, MDA-MB-231 and HDF cell-lines were seeded at a density of 15 000 cells per gel. The PA gels with cells were incubated for 24 hours before imaging. To image, a brightfield and a fluorescent image were taken before and 15 minutes after releasing the cells from the gel using 10x trypsin.

Analysis. Images were analysed using Fiji ImageJ software and statistics were performed using GraphPad Prism (p-values determined by Kruskal-Wallis test).

RESULTS: Fibroblasts contract the gel by 60% over 24 hours. MDA-MB-231 cells contract the gel by 22% over 24 hours. HT-29 and HCT 116 cancer cells did not contract the gel, regardless of cell concentration and time. TFM results validate this trend. A HDF cell displaces the matrix by 3 µm on average. An MDA-MB-231 cell displaces the matrix by 1 µm. HCT116 and HT-29 cells do not displace the matrix.

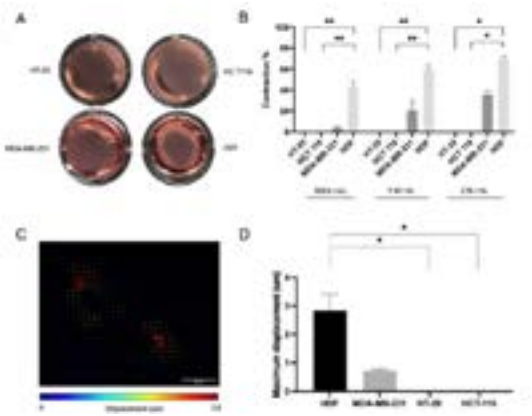

Fig. 1: A. Images of the collagen hydrogels after 24 hours at 1 M/mL cells. B. Contraction of the hydrogels after 24 hours. C. Displacement field of an MDA-MB-231 cell. D. Displacement in µm of the matrix by each cell type.

DISCUSSION & CONCLUSIONS: Both methods show that epithelial colorectal cancer cells such as HT-29 and HCT 116 do not contract the local matrix or surrounding stroma whilst breast cancer cells MDA-MB-231 have the ability to do so. This demonstrates that, within this instance, breast cancer cells have a stronger propensity to interact with the ECM. Their ability to contract the matrix suggests that they can remodel collagen fibres, aiding cancer growth and invasion. This suggests a mesenchymal phenotype directly related to their highly metastatic and aggressive nature.

ACKNOWLEDGEMENTS: This template was modified with kind permission from eCM conferences Open Access online periodical & eCM annual conferences. We are grateful for supports from UCL Institute of Healthcare Engineering and EPSRC DTP PhD Studentship (EP/R513143/1).

A novel preservation technique for the manufacture of biocompatible and terminally-sterilised transplantable human corneas

E.R. Britchford[1,2], L.J. Beeken[1], O.D. McIntosh[1], A. Hopkinson[1,2], L.E. Sidney[1]

[1]*Academic Ophthalmology, Division of Clinical Neuroscience School of Medicine, University of Nottingham, Nottingham, England, UK, 2 NuVision Biotherapies Ltd, Nottingham , UK*

INTRODUCTION: Approximately 185,000 corneal transplants are performed annually in 116 countries, thus leaving over 12 million corneal-blind cases worldwide untreated. One of the biggest limitations to corneal transplantation is access to quality donor tissue due to inadequate eye donation services and infrastructure in developing countries. This is compounded by the fact that there are no long-term storage solutions for effectively preserving spare donor corneas collected in countries with a surplus. Eye banking infrastructure requires large amounts of local investment and labour to put in place, however, increased access to tissue can be achieved by development of preservation techniques to increase corneal storage times and allow for global shipping at ambient temperature. This preservation will also allow storage on hospital shelves, for use in emergencies, where waiting for donor corneas is not possible.

METHODS: A novel, patented [1], drying technique was used to preserve human corneas collected in the US and UK, that were deemed unsuitable for transplantation (figure 1). We assessed weight, thickness, transparency, cell viability, cell membrane permeabilisation, ECM content and structure, comparing to non-dried donor corneas. Biocompatibility and cell integration was assessed by co-culture with human corneal cells and a subcutaneous implantation model in rats. Effects of gamma-irradiation, as a terminal sterilisation procedure, on the structure of the dry corneas was assessed using histology, ELISAs and collagen quantification.

RESULTS: The dried corneas were comparable to non-dried donor corneas in all investigated aspects except cellular viability. When implanted subcutaneously in rats, the dried cornea was well tolerated, with cellular migration into the matrix. Biocompatibility tests with human corneal cells demonstrated no adverse effects. Gamma-irradiation at 25kGy had no detrimental effect on cornea structure or protein composition.

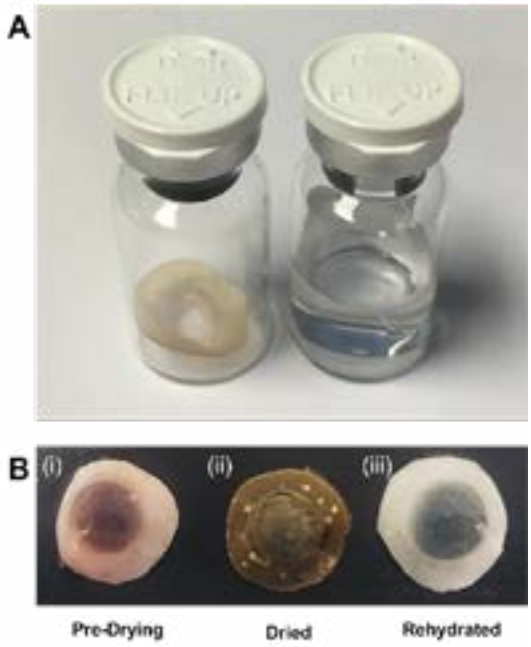

Figure 1. ***(A)*** *Dried corneas as currently manufactured, dried in glass vials and supplied with a clear rehydration solution.* ***(B)*** ***(i)*** *Donor cornea supplied by SightLife;* ***(ii)*** *Cornea after preservation by drying;* ***(iii)*** *Dried cornea after rehydration.*

DISCUSSION & CONCLUSIONS: Our preservation technique provides an easy-to-manufacture, non-viable, dehydrated, cornea suitable for a range of clinical indications and tectonic support in emergency situations. It can be stored on the shelf in hospitals for over 2 years and can be shipped at ambient temperatures worldwide, relieving the global shortage of corneal tissue.

ACKNOWLEDGEMENTS: Funded by an MRC CiC award, EPSRC IAA Award and Innovation and Knowledge Centre (IKC) for Medical Technologies Proof-of-Concept award.

REFERENCES: [1] Sidney LE, Hopkinson A, McIntosh OD, UK Intellectual Property Office 2020; PCT/GB2020/052906.

DEVELOPING A HYDROGEL-ASSISTED COMBINATION THERAPY FOR BRAIN REPAIR FOLLOWING ISCHAEMIC STROKE

R. Sava[1], R. Wong[1], C. Albornoz[1], C. Ligorio[1,2,3], A. Saiani[2,3], J. Penny[1], S. Allan[1], E. Pinteaux[1]

[1]Faculty of Biology, Medicine and Health, The University of Manchester [2] Manchester Institute of Biotechnology, The University of Manchester [3]Faculty of Science and engineering, The University of Manchester

INTRODUCTION: With no available treatments for brain tissue repair and functional recovery in patients with lost or impaired neurological functions, stroke therapy remains an important unmet clinical need. The lack of structural support in the stroke cavity resulting from dead tissue clearance by immune cells and insufficient endogenous tissue repair dramatically limit brain functional recovery after stroke. These two factors are potential targets to be considered when designing novel regenerative therapies[1]. For example, soft hydrogels may offer the necessary structural support and deliver pro-regenerative therapeutic agents for improving their half-life[1,2]. To explore a novel hydrogel-based combination therapy, we tested the biocompatibility with the brain tissue of a novel self-assembling peptide hydrogel (SAPH), and its capacity to release vascular endothelial growth factor (VEGF). Furthermore, we have assessed the reparative properties of tumour necrosis factor-alpha stimulated protein-6 (TSG-6), a multifunctional protein with anti-inflammatory properties[3].

METHODS: To study its brain biocompatibility, the PeptiGel-Alpha2 hydrogel was injected intra-cerebrally in healthy mouse brains. Microglial activation as a measure of brain inflammation, as well as phagocytosis were assessed by immunohistochemistry (IHC). Levels of recombinant human VEGF (rhVEGF) released by the hydrogels for six weeks were assessed by enzyme-linked immunosorbent assay. To study the therapeutic effect of TSG-6 in a mouse model of ischaemic stroke, rhTSG-6 was injected intra-cerebrally 5 days post-stroke, and wellbeing and motor asymmetry were assessed up to 28 days post-stroke. Markers associated with brain inflammation, angiogenesis and neurogenesis were assessed by IHC on brain sections.

RESULTS: The PeptiGel-Alpha2 hydrogel, did not induce microglial activation, therefore is biocompatible with the brain tissue. In contrast, the hydrogel induced the recruitment of phagocytic cells, indicating a clearing mechanism. Moreover, the hydrogel released rhVEGF in a sustained manner *in vitro*, and ongoing experiments are testing the bioactivity of this angiogenic growth factor. These findings support the use of PeptiGel-Alpha2 as a temporary scaffold for brain repair and VEGF release system. In parallel, our *in vivo* study revealed a trend toward improved wellbeing, decreased microglial activation, increased endothelial cell proliferation, and increased number of neuroprogenitor cells following rhTSG-6 administration into the stroke cavity. This indicates that TSG-6 has beneficial tissue repair properties post-stroke.

CONCLUSIONS: Our work describes a novel brain biocompatible SAPH hydrogel with VEGF release capacity suitable for angiogenic applications following brain injury. In parallel, we have tested for the first time the reparative properties of TSG-6 administered sub-acutely in the stroke infarct, and the results have shown the potential this anti-inflammatory and pro-regenerative protein has as a therapeutic tool for stroke. Ongoing work is testing the efficacy in stroke of TSG-6 and VEGF combination, assisted by a SAPH-based delivery system. The functional recovery and tissue repair will be assessed 28 days post-stroke. The findings of this study will reveal the therapeutic potential of VEGF/TSG-6/PeptiGel-Alpha2 hydrogel combination for structurally supporting tissue repair and promoting functional recovery after stroke.

REFERENCES:

1. Nih, L. R., *et al*. Curr. Opin. Biotechnol. **40**, 2016.
2. Mohtaram, N. K., *et al*. Biomed. Mater. **8**, 022001, 2013.
3. Day, A. J. & Milner, C. M. Matrix Biol. **78–79**, 60–83, 2019.

Semi-artificial pancreas for the treatment of Type 1 diabetes: Perspectives, challenges, and solutions

J. Hinchliffe[1*], D. A. Gregory[1], I. Roy[1].

[1]*Department of Materials Science and Engineering, Faculty of Engineering, University of Sheffield, UK*

INTRODUCTION: Type 1 diabetes is an autoimmune condition which, through a pathological immune system action enables the destruction of the β-cells of the pancreatic islets of Langerhans, reducing insulin production capacity[1]. A proposed replacement for insulin injections and pancreas transplants is the production of a bioartificial pancreas, with which will include immune-isolated islets, such that immune cells and their cytotoxic products are denied access to the implanted tissue [2]. Polyhydroxyalkanoates (PHAs) are becoming known in biomedical applications due to their tunable properties, non-immunogenicity, and relative biocompatibility with multiple tissue types[3]. This work aims to generate a 3D-printable bioartificial scaffold for islets, using bioresorbable bacteria-derived polymers such as alginate and PHAs.

METHODS: The elastomeric PHA, poly (3-hydroxyoctanoate-*co*-3-hydroxydecanoate), was produced via bacterial fermentation using a *Pseudomonas sp.* over a 24-hour period. After centrifugation and freeze drying, the cells were subjected to Soxhlet extraction to obtain pure polymer. The exact chemical structure of the polymer was confirmed using Gas Chromatography-Mass Spectrometry. Polymer films were made using the solvent casting process and seeded with BRIN-BD11, a pancreatic beta cell line, using the resazurin viability assay to determine cytocompatibility. Fused Deposition Modelling (FDM) was used to create multi-material, high-fidelity artificial pancreas constructs where a P(3HO-co-3HD) external structure mechanically supports discrete amounts of alginate containing encapsulated islets (Figure 1a).

RESULTS: Initial findings showed that P(3HO-*co*-3HD) was a better substrate for the BRIN-BD11 cells as compared to Poly(3-hydroxybutyrate), a stiff PHA, Polycaprolactone, alginate and TCP using the resazurin assay. 3D printed multi-material constructs were successfully produced using P(3HO-*co*-3HD) and alginate. Mechanical testing of these constructs indicated that the P(3HO-*co*-3HD) strut size in the structure affected the construct elasticity, with 200μm diameter struts displaying higher elasticity compared to larger diameters and were closer to the mechanical properties of the pancreas[4].

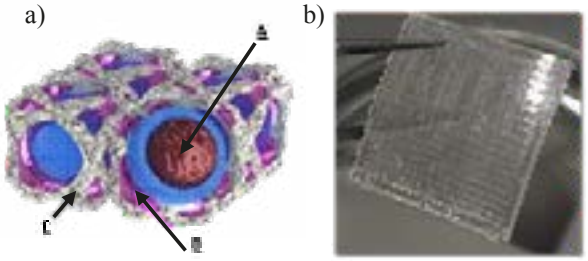

Fig. 1: a) A proposed model for the bioartificial pancreas, containing whole islets (A) in an immunoisolating alginate matrix (B), mechanically protected by a P(3HO-co-3HD) scaffold (C) (b) A FDM printed P(3HO-co-3HD) and alginate multimaterial construct.

DISCUSSION & CONCLUSIONS:
The cell behaviour analysis demonstrated that both P(3HO-*co*-3HD) and sodium alginate were highly biocompatible with BRIN-BD11 cell lines *in vitro*, holding promise for the eventual translation into the use of rat and human primary islet tissue. In future work will be undertaken to better understand the effect of bioprinting within the final P(3HO-*co*-3HD) construct. We also aim to functionalise the polymer for improved vascularisation and immune barrier function in the *in vivo* environment.

ACKNOWLEDGEMENTS: We thank Prof. Victor Gault and Prof. Nigel Irwin from Ulster University for their advice and the gift of BRIN-BD11. We also thank the University of Sheffield and EPSRC for JH's scholarship.

REFERENCES:

1. Atkinson et al., 2014. Type 1 diabetes. The Lancet, 383(9911), pp.69-82. 2. Nafea et al.,2011. Immunoisolating semi-permeable membranes for cell encapsulation: focus on hydrogels. Journal of controlled release, 154(2), pp.110-122. 3. Zhang et al., 2018. Polyhydroxyalkanoates (PHA) for therapeutic applications. Materials Science and Engineering: C, 86, pp.144-150.4. Nicolle e al., Shear mechanical properties of the porcine pancreas: Experiment and analytical modelling. Journal of the mechanical behavior of biomedical materials, 26, pp.90-97.

Utilising human tissue-engineered skin equivalents to determine chemical irritation potential

HARDING AL[1], Murdoch C [1], Danby S [2], Hasan MZ [3], Nakanishi H [3], Furuno T [3], Hadad S [4], Turner R [5], Colley HE [1].

[1]School of Clinical Dentistry, University of Sheffield, Sheffield, UK. [2] Sheffield Dermatology Research, Department of Infection, Immunity & Cardiovascular Disease, Medical School, University of Sheffield, Sheffield, UK. [3]Rohto Pharmaceutical Co., Ltd., Safety Design Centre, Kyoto, Japan. [4]Sheffield Teaching Hospitals NHS Foundation Trust, Sheffield, UK. [5]Research Software Engineering Team, University of Sheffield, UK.

INTRODUCTION: Adverse skin sensation in response to topical product use is a common reason for poor treatment compliance. The aim of this study was to develop novel tissue-engineered skin equivalents that are able to predict stinging potential *in-vitro*.

METHODS: Human skin equivalents (HSE) were generated by embedding primary or immortalised dermal fibroblasts in a collagen hydrogel and culturing hTERT-immortalised skin keratinocytes on top at an air-to-liquid interface for 14d. Stinging reagent lactic acid (LA; 5%), or cosmetic chemicals methyl-paraben (MP, 0.2%) cocamide diethanolamine/monoethanolamine (Co-DEA/MEA; 2%) were added topically to HSE or *ex-vivo* skin explants for 24h. Their gene signatures determined for known irritants and non-irritants determined using qPCR and multivariate analysis; by heat-map generation and principal component analysis (PCA). Suitability of HSE for high-throughput testing was accomplished using linear discrimination analysis (LDA) using R-Studio software.

RESULTS & DISCUSSION: In HSE, LA treatment resulted in a significant fold increase in STAT1, MAP3K8, TAC-1 expression, as well as HSP1A and MMP-3. No significant observations were made with MP or Co-MEA treatment, however, HSP1A expression significantly increased with Co-DEA treatment (Figure 1a). Hierarchical clustering of gene expression data followed by PCA revealed that this 22-gene panel could effectively discriminate between LA and the non-irritants MP, Co-DEA, and Co-MEA. The non-irritants clustered closely together for both HSE *and ex vivo* skin, whereas gene responses to LA clustered into two distinct clusters, one for HSE and one for skin (Figure 1b). Linear discrimination analysis (LDA) identified seven genes with coefficients above 0.5 (*IL-6, PTGS2, ATF3*, *TRPV3, MAP3K8, HMGB2*, and *MMP-3*) that were then re-analysed for their hierarchical clustering profiles and PCA. Confirming they retained their ability to discriminate irritant from non-irritant chemicals.

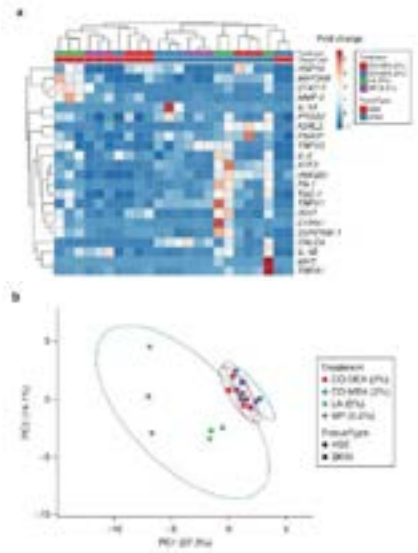

Fig. 1: Multivariate analysis of chemical stimulation on gene signatures in skin and HSEs. Unsupervised hierarchical clustering of gene expression data for 22 genes after treatment with chemicals (a). PCA representing gene expression profiles for skin (square) and HSE (circle). The score plot displaying PC1 and PC2 explains 37.3% and 14.1% of the total variance, respectively, after exposure (b).

CONCLUSION: The expression of a seven-gene panel in HSE, based on immortalised keratinocytes, in combination with multivariate statistical approaches shows enhanced confidence in the discrimination of skin irritants from non-irritants.

ACKNOWLEDGEMENTS: Ms. K D'Apice for her assistance with tissue collection.

Investigating the use of single material 'composite' alginate scaffolds for cartilage tissue engineering

A.Sturtivant, A.Callanan

Institute of Bioengineering, School of Engineering, University of Edinburgh, United Kingdom

INTRODUCTION: At present osteoarthritis is a leading cause of disability worldwide. Cases are predicted to double to more than 17 million cases per year by 2030[1]. Current medical approaches seek to replace large regions of anatomy in invasive surgeries as treatments. While effective, these options have limited lifespans, needing revision surgeries, or are not suitable for younger patients. New tissue engineering approaches aim to permanently regenerate damaged regions of the body to mitigate the need for multiple surgeries[2]. Here we present a method for forming scaffolds with structurally distinct regions in an effort to recapitulate the native cartilage structure and observe cell response.

METHODS:
A 2.5% w/v alginic acid solution was combined with equal parts Methacrylic Anhydride and reacted at pH 7 for 72 hours under constant stirring. This was then dialysed and freeze dried. Functionalised Alginate (AlgMA) was made into a solution of 4% w/v. 0.1mg/mL igracure 2959 was then added as a photoinitiator. This solution was crosslinked using a 365nm light. This was then placed on a cold plate before being placed in a freeze dryer to create directional pores. Hydrogel groups were formed by crosslinking the precursor solution as above, either alone or onto the pre-fabricated sponges. Scaffolds were characterised using SEM and Instron Compression testing. Native Bovine Chondrocytes were also harvested and seeded into the scaffolds with viability and Chondrogenesis being assessed over 21 days.

RESULTS:
Results showed it was possible to fabricate sponges and gels, and combine them into a single crosslinked unit. These constructs had varying mechanical properties and while maintaining cell viability demonstrated varying phenotypic responses.

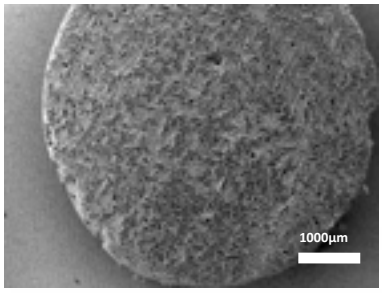

Figure 1 - SEM image of ALGMA scaffold.

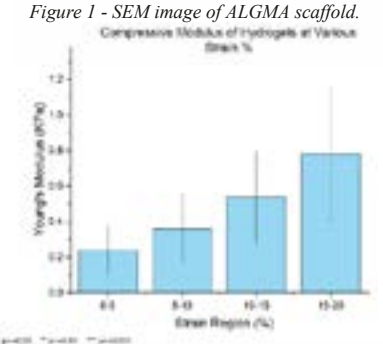

Figure 2 – Mechanical properties of AlgMA gel..

DISCUSSION & CONCLUSIONS:

We demonstrated that the 2 regions differ mechanically, and structurally, but maintained chondrocyte viability and phenotype over 21 days, with positive trends observed in DNA and GAG content. This shows it was possible to combine hydrogel and sponge scaffolds, both fabricated from alginate, into single units, with regionally distinct microstructure that mimcs the native articular cartilage.

ACKNOWLEDGEMENTS: This work is funded by an Engineering and Physical Sciences Research Partnership Studentship (grant number: EP/R5132091).

REFERENCES:

[1] Conaghan, P.G., et al. Impact and therapy of osteoarthritis: the Arthritis Care OA Nation 2012 survey. 2012.
[2] Musumeci G, et al. New perspectives for articular cartilage repair treatment through tissue engineering: A contemporary review. 2014.

Bioengineering a 3D tissue model of the rectus sheath to study herniation

A. Grillo[1], M. Caluianu[1], A. Barna[1], V. Mudera[1], A. Kureshi[1]

[1] *Centre for 3D Models of Health and Disease, Division of Surgery and Interventional Science, University College London, London, UK*

INTRODUCTION: Posterior rectus sheath is a highly aligned connective tissue with collagen fibres aligned in the transverse direction and it is the layer mostly involved in hernia formation [1]. Current meshes used for hernia repair which include biological components, do not mimic the anisotropic structure of the rectus sheath, which could explain the possible failure of the implant. The aim of this study is to develop a 3D tissue model of the rectus sheath which mimics the alignment of the collagen fibres in the native tissue.

METHODS: Gels were prepared by adding 3.7 ml of Type I rat tail collagen to 0.36 ml 10x MEM and neutralising with 0.191 ml of neutralising solution, with the final addition of 0.193 ml of DMEM. Once set, the fluid was removed from the gels using the RAFT process coupled with a novel mechanical shear flow technique (manuscript in preparation) [2]. Human Dermal Fibroblasts (HDFs) were seeded on top of the constructs to indirectly evaluate the collagen fibres orientation. Gels were fixed and stained with Phalloidin and DAPI to visualize the nuclei and the cytoskeleton. Their angle of orientation was measured via ImageJ. Control unaligned gels were represented by standard RAFT constructs.

RESULTS: Anisotropic gels were successfully manufactured and HDFs were seeded on top and cultured for 1, 2 and 4 days. Fig, 1 (left) shows that overall HDFs were oriented according to the direction of alignment (indicated by the yellow arrow). Quantitative analysis was performed and the graph in Fig. 1 (right) shows the angle of orientation over time, compared to that of HDFs seeded on isotropic RAFT constructs. In particular, the mean orientations for aligned constructs were 21.0 ± 9.1˚, 18.8 ± 4.7˚ and 18.5 ± 12.5˚, for 1, 2 and 4 days, respectively. For each time point, the orientations on aligned constructs are significantly different from those on the unaligned RAFT constructs (***p<0.001, **p<0.01), with no significant difference in mean orientation among the three different time points.

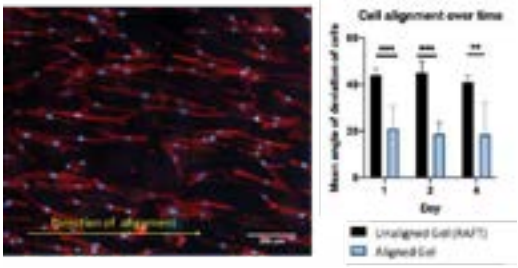

*Fig. 1: Immunofluorescence image of HDFs on aligned gel (left) and graph representing the mean orientation of HDFs over time (1, 2, 4 days) (right). RAFT N=4, Aligned gels N=6-9. Anova test, ***p<0.001, **p<0.01.*

DISCUSSION & CONCLUSIONS: Numerous techniques such as GAE and tethering gels have been used to create aligned collagen constructs [3] [4]. However, these techniques either do not produce flat sheets of collagen or they require the use of cells to align the structure. This technique would rapidly produce a 3D model of the rectus sheath which will allow us to study the biology of herniation, once populated with primary healthy and hernia fibroblasts. Moreover, this model is highly tuneable and could be used to mimic different tissues with similar aligned structure (tendon, nerve, cornea). Further analysis of the collagen fibres orientation and comparison with the native tissue will be performed to validate the model.

REFERENCES:

1. Axer, H., D.G.v. Keyserlingk, and A. Prescher, *Collagen Fibers in Linea Alba and Rectus Sheaths: I. General Scheme and Morphological Aspects.* Journal of Surgical Research, 2001. **96**(1): p. 127-134.
2. Levis, H.J., et al., *Tissue Engineering the Cornea: The Evolution of RAFT.* J Funct Biomater, 2015. **6**(1): p. 50-65.
3. Kamranpour, N.O., et al., *A gel aspiration-ejection system for the controlled production and delivery of injectable dense collagen scaffolds.* Biofabrication, 2016. **8**(1): p. 015018.
4. Georgiou, M., et al., *Engineered neural tissue for peripheral nerve repair.* Biomaterials, 2013. **34**(30): p. 7335-43.

The thickness of soft hydrogel substrates modifies bone marrow stromal cell morphology and differentiation

M. L. Hernandez[1], B.G. Sengers[2], N.D. Evans[1,2]

1Centre for Human Development, Stem Cells and Regeneration, Human Development and Health, Institute of Developmental Sciences, 2Mechanical Engineering, University of Southampton, Southampton, United Kingdom

INTRODUCTION: The elastic modulus of growth substrates and/or extracellular matrix affects the spreading, proliferation and differentiation of many cell types, including bone marrow stromal cells (BMSC). However, the stiffness that cells sense is determined not only by substrate modulus, but also by geometry, such as material thickness. In this study, we hypothesised that BMSCs would spread, proliferate and differentiate to the osteogenic lineage to a greater degree as the thickness of soft materials (*E* ~1kPa; adhered to a rigid substratum) decreased.

METHODS: We fabricated polyacrylamide hydrogel matrices of different stiffness ranging from 1 to 40 kPa. We also modified the 1KPa hydrogels by varying the polyacrylamide mixture volume (5 - 100 µL). Hydrogels stiffness was measured by nanoindentation while thickness was measured by confocal microscopy (Leica SP8 microscope). Type I (atelo-) collagen at a concentration of 0.1 mg/cm^2 was covalently linked to the hydrogels. BMSCs were seeded at various densities to evaluate the effect of stiffness or thickness. Cells were then stained with DiD and imaged using a Ti-Eclipse Nikon inverted microscope and single cell spreading area was measured. Focal adhesions were detected by immunocytochemistry (Vinculin Polyclonal Antibody, Goat anti-Rabbit IgG, Alexa Fluor 594, Fisher scientific) Osteogenic differentiation was assessed in cells grown (5,000 cells/cm^2) for 7 and 14 days in αMEM, with or without ascorbate, betaglycerophosphate and dexamethasone. Cells were stained with Fast Violet (Sigma) for Alkaline Phosphatase (ALP) activity and nuclei was staining with DAPI. Additionally, we evaluated deformations on soft and stiff gels of different thickness containing fluorescent beads, 0.5µm in basal and osteogenic conditions by time-lapse imaging (Ti-Eclipse Nikon inverted microscope) and an algorithm based on spatial cross-correlation between sequential images.

RESULTS: 1 kPa hydrogels were thicker than 40 kPa. (~1200 µm and ~623 µm respectively for a polyacrylamide volume of 100 µL). Also, the elastic modulus of soft and stiff gels increases on thinner hydrogels; ~19kPa (5µL) vs ~5kPa (50µL) for soft and ~200µm (5µL) vs ~60µm (50µL) for stiff gels. BMSC grown on thick soft gels spread to a lesser extent than those on thin gels with a mean cell area of 2600 ± 79 and 5600 ± 990 µm^2 respectively. Quantification of displacements revealed greater deformations of soft thick (~32 pixels) and soft thin (~19 pixels) in basal media compared to soft thin and thick hydrogels (~14 and ~10 pixels) in osteogenic media. In contrast, small deformations were found on stiff gels (~3 pixels) regardless of their thickness or media conditions. In additional experiments, we confirmed that soft gels deformed significantly during cell spreading process just after seeding, and that these hydrogel deformations might be irreversible after cell detachment. Cell proliferation and osteogenic differentiation was promoted on stiff gels; however a decrease on thickness enhanced osteogenic differentiation on soft gels Focal adhesions were distributed evenly in cells on stiff substrates or on plastic regardless of thickness, and defined actin fibres were always prominent (On soft materials FAs were found near the nucleus and no clear actin fibers were observed on soft gels.

DISCUSSION & CONCLUSIONS: The observation that stiffer and soft thin hydrogels promote cell spreading, cell proliferation and differentiation and focal adhesions formation suggest that an overall increase in substrate stiffness by the increase in intrinsic elastic modulus and decrease in thickness modifies cell behaviour as the cells might be able to 'feel through' the soft gel to the underlying glass substrate. This may suggest that by modifying the substrate thickness it would be possible to modify cell morphology and consequently promote differentiation for tissue repair.

ACKNOWLEDGEMENTS: CONACyT, Mexico), University of Southampton, UK.

REFERENCES: Engler et al., 2006. Matrix elasticity directs stem cell lineage specification. //Tusan CG, Hin Y, Zarkoob H, Johnston D, Andriotis OG, Thurner PJ, Yang S, Sander EA, Gentleman E, Sengers BG, Evans ND. (2018). Collective Cell Behavior in Mechanosensing of Substrate Thickness. Biophysical Journal 114, 2743–2755, June 5, 2018.

Hydrogels characterization for Skeletal Muscle Regeneration

F. Carton[1], D. Di Francesco[1], F. Boccafoschi[1]

[1]*Department of Health Sciences, University of Piemonte Orientale 'A. Avogadro', 28100 Novara, Italy.*

INTRODUCTION: Skeletal muscles represent 40% of body mass and it can be damaged by tumour removal, traumatic injuries and diseases. Typically, smaller injuries are repaired by the body through the activation of satellite cells while traumatic injuries such as congenital abnormalities, denervation or tumour ablation lead to the loss of muscle functions. Although great efforts have been dedicated to better understand the mechanisms controlling muscle regeneration, few attention have been paid on the clinical approaches used to treat muscle injuries and wasting (1). To date, tissue engineering could represent a promising strategy for regenerating the lost tissue (2). This study characterized the morphological and molecular features of C2C12 myotubes cultured on natural hydrogel obtained from the decellularization of bovine pericardium (dECM).

METHODS: Hydrogel have been obtained from decellularized bovine pericardium (dECM) (Tissuegraft srl). C2C12 myotubes were grown on different coatings (4 mg/mL of dECM, 1.6 mg/mL of collagen and traditional plasticware) in order to study their effect on myotube formation during the differentiation time course (days 3, 6, 9, 12). The effect of each coating on myotubes morphology, viability and differentiation was measured by fluorescence images, MTT assay, and image analysis. In order to characterize the ability of maintain a contractile phenotype, western Blot analyses have been performed.

RESULTS: The number of myotubes grown on dECM hydrogel were quantitatively higher compared to the cells differentiated on plastic and collagen (Fig. 1). To further assess myotubes formation, the average width of cells growth on the different substrate was also measured. At day 9, myotubes were wider on dECM hydrogel compared to the others conditions suggesting that the long-term adhesion and morphology was improved by dECM stimuli. Finally, the ability of dECM to support myogenesis was assessed by measured the expression of specific myogenic markers: Myogenin and myosin heavy chain (MHC). In particular, results showed that cells grown on dECM hydrogel expressed higher amount of myogenin at day 6 (Fig. 2) while MHC, a marker of mature myotubes, was highly expressed at day 9 (data not shown).

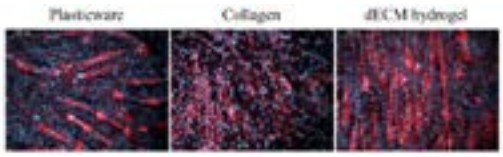

Fig. 1: Representative images of C2C12 myotubes formation: DAPI (blue), phalloidin (red). Magnification 10X.

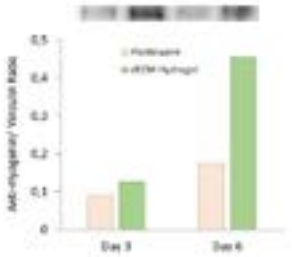

Fig. 2: Representative western blot of myogenin content.

DISCUSSION & CONCLUSIONS: Our data showed that C2C12 myoblasts were able to differentiate on dECM hydrogel yielding a more fully matured myotube culture. Cellular width and myogenic markers, suggest an increase in myotubes formation on dECM hydrogel with a higher level of maturity. Thus, hydrogel systems could represent an attractive and simple approach to overcome the problems related to the lost muscle, to restore function and increase patient quality of life.

ACKNOWLEDGEMENTS: The authors would like to thank Tissuegraft srl, 28100 Novara (Italy) that support this work.

REFERENCES: [1] R. Lev. et al. J R Soc Interface 2018, 15(138):20170380.
[2] L.T. Denes et al. Skelet Muscle 2019, 9(1):17.

Self-assembling Nanoclay gels with 3D Micropatterning of BMP-2 for Bone Tissue Regeneration

R.S. Ramnarine [1], N. Evans [1], R.O.C. Oreffo [1], J. Dawson [1].
[1]*Bone & Joint Research Group, Centre for Human Development, Stem Cells & Regeneration, Institute of Developmental Sciences, University of Southampton, Southampton, SO16 6YD, United Kingdom.*

INTRODUCTION: Emulating the three-dimensional (3D) organization of biochemical cues present in the native cellular microenvironment is likely to be key to generate biomaterials with distinct levels of functionality. However, despite advances in tissue engineering (TE), building structures incorporating stable 3D-micropatterning of biochemical cues and that preserve their resolution with an increase in size has proven challenging[1]. Nanoclay-gels have established potential in TE due to their capacity to adsorb, retain and localize proteins bioactivity[2]. The current study reports a novel and simple method to applying nanoclay-gels for spontaneous 3D micropatterning of proteins, supporting the delivery of localized stable niches for enhanced bone regeneration.

METHODS: Suspensions of a synthetic smectite clay (Laponite®), were exposed to a solution containing biomolecules and ions present in blood plasma to support the self-assembly of micro-patterned scaffolds through a reaction-diffusion process. The assembled structures were tested for their ability to pattern fluorescently-labelled model proteins (albumin, avidin, streptavidin, immunoglobulin, casein) and to localize the activity of bone morphogenetic protein (BMP-2) The structures were analysed using a range of imaging techniques, including fluorescent, polarized light and electron microscopy, and a 28-day murine subcutaneous implantation assay.

RESULTS: Nanoclay/protein scaffolds develops an internal degree of order that allows templating punctuated or gradual 3D gradients of all proteins. By changing parameters known to affect diffusion rate at the assembly step, such as concentration, ionic strength, incubation time and temperature, it was possible to demonstrate control over the spatial localization of the proteins. With this method is possible the assembly of structures at scale with a range of dimensions (0.2 - 1mm) and shapes (droplets, cylinders, strings) while preserving the resolution of protein patterning. The assembled structures displayed a radial birefringence under polarized light, indicating the presence of periodical arrangements of nanoparticles. Finally, the *in vivo* study revealed that punctuated localisation of BMP-2 within the scaffold provided the potential to control the spatio-temporal formation of mature bone.

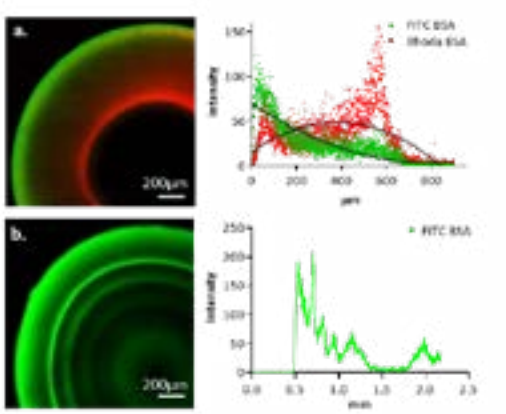

Figure 1: Self-assembled nanoclay/protein scaffolds containing different protein patterns: a) simultaneous positive and negative gradients of BSA. b) multiple BSA patterns.

DISCUSSION & CONCLUSIONS: We demonstrated for the first time the potential to harness interactions between clay-nanoparticles and biomolecules present in physiological fluids to design scaffolds with complex biochemical gradients, dimensions and shapes for bone with clinical relevance.

ACKNOWLEDGEMENTS: Funded by EPSRC (EP/L010259/1 and EP/S017054/1) and University of Southampton, postgraduate awards to JI Dawson.

REFERENCES

[1] Wylie RG, et al. Nat. Mater. 2011; 10: 799-806.
[2] Dawson JI, et al. Adv. Mater. 2013; 23: 3304-3308

Bioprinting the Hierarchical Extracellular Matrix Environment for Articular Cartilage Repair

S. A. Read[1], A. G. Dumanli-Parry[2], S. J. Kimber[3], M. Domingos[1]

[1]Department of Mechanical, Aerospace and Civil Engineering, Faculty of Science and Engineering & Henry Royce Institute, The University of Manchester. [2]Department of Materials, Faculty of Science and Engineering & Henry Royce Institute, The University of Manchester. [3]Division of Cell Matrix Biology and Regenerative Medicine, Faculty of Biology, Medicine and Health, The University of Manchester

INTRODUCTION: Articular cartilage (AC) damage can result in osteoarthritis – one of the leading causes of joint immobility. Current clinical therapies are insufficient in regenerating AC for long-term success. The collagen fibre network of AC provides the tissue with depth- and directional-dependent biomechanical properties that are fundamental in its function. Recapitulating this framework *in vitro* still proves challenging. Cellulose nanocrystals (CNCs) self-assemble in a hierarchical fashion similar to collagen architectures. We hypothesise that CNCs can be combined with a hydrogel to create bioinks capable of (1) supporting chondrogenic differentiation of human pluripotent stem cells (hPSCs) and (2) direct the alignment of newly-synthesised collagen fibrils for improved biomechanical performance of AC implants.

METHODS: CNCs were extracted and purified as described by Dumanli *et al*., and characterised using conductometric titrations.[1] A LIVE/DEAD assay was performed on an immortalised chondrocyte line (TC28a2) seeded on 2D CNC films to obtain a preliminary evaluation of biocompatibility. CNCs were combined with alginate at final concentrations of 5% (w/v) and between 0.5-1.0% (w/v), respectively. Crosslinking was achieved by immersion in 150 mM $CaCl_{2(aq)}$ for 10 mins. Oscillatory rheology was used to determine the mechanical properties of the formulated hydrogel systems.

RESULTS: A large proportion of live cells were seen on 2D CNC films after 24 h. Independent of alginate concentration or CNC presence, all hydrogels displayed a dominant elastic behaviour. Increasing the alginate concentration from 0.5% (w/v) to 1.0% (w/v) increased the storage and loss modulus by over 2x, while adding 5% (w/v) CNCs appears to increase the storage modulus by just over half. While CNCs did not extend the LVE region significantly, they increased the yield stress of the hydrogels (solid-liquid transition). (Fig. 1)

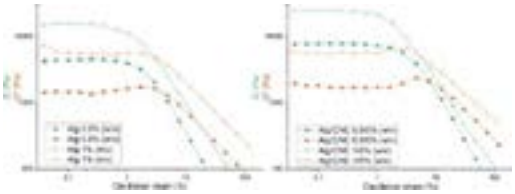

Fig. 1: Storage (G') (green) and loss (G'') (orange) modulus graphs for 0.5/1.0% (w/v) alginate (left) and the same formulations with the addition of 5% (w/v) CNC (right).

DISCUSSION & CONCLUSIONS: Initial results suggest that CNCs do not affect cell viability. Adding 5% (w/v) CNCs improves the elastic behaviour of alginate, thus suggesting improved stability under mechanical loading. Future work includes polarised microscopy and diffraction experiments to elucidate CNC self-assembly within the hydrogels. TC28a2 cells will be used to confirm CNC/alginate biocompatibility using LIVE/DEAD assays and to assess the effect on chondrogenic gene expression using RT-qPCR. Later, the effect of CNCs on hPSCs chondrogenic differentiation, using a protocol similar to Wang *et al*., will be studied.[2] It is hoped that CNCs can provide an alternative means to generating intricate collagen architectures within 3D hydrogel constructs for tissue engineering and disease modelling applications.

ACKNOWLEDGEMENTS: S. A. Read is supported by the EPSRC Centre for Doctoral Training in Advanced Biomedical Materials.

REFERENCES: 1. Dumanli A *et al*. Optical Mater. 2: 646-650, 2014. 2. Wang T *et al*. Stem Cell Res. 39:101497, 2019.

Assessment of the Therapeutic Potential of Corneal Mesenchymal Stem Cells for Ocular Surface Disorders

Lydia Beeken[1], Cameron Alexander[2], Felicity Rose[3], and Laura Sidney[1]
[1] Academic Ophthalmology, Division of Clinical Neuroscience, School of Medicine, University of Nottingham, Nottingham, NG7 2UH. [2] School of Pharmacy, Boots Science Building, University Park, Nottingham, NG7 2RD. [3]School of Pharmacy, Biodiscovery Institute, University Park, Nottingham, NG7 2RD.

INTRODUCTION: Following severe mechanical or microbial insult to the cornea, the destructive acute inflammatory phase can activate the transformation of keratocytes to scar-forming fibroblasts, causing significant corneal opacity. Although blindness can be reversed with corneal transplant, excessive inflammation leads to surgery waiting times of up to 18 months. Corneal stromal mesenchymal stem cells (C-MSCs) have previously been identified to possess potent anti-inflammatory properties [1], and their incorporation into a regenerative medicine therapy has potential to combat the acute inflammation and reduce the wait for surgery. To ensure success in terms of clinical translation, it is vital to understand the tolerance and response of C-MSCs when placed in the toxic microenvironment of an injured ocular surface. This includes determination of any phenotypic and genotypic changes, in addition to assessment of their survival, behaviour and anti-inflammatory response.

METHODS: C-MSCs were isolated from human corneoscleral rims. An *in vitro* inflammatory environment, typical at a site of injury, was created through incorporation of TNF-α, IFN-γ, IL-1β and LPS into the medium. Cell response was analysed through immunocytochemistry, ELISAs, and Live/Dead, PrestoBlue and cytotoxicity assays. The BD Lyoplate™ Human Cell Surface Marker Screening Panel was utilised to determine any changes of the C-MSC phenotypic profile in the different conditions.

RESULTS: Inflammatory cocktail addition reduced cell survival, however the remaining C-MSCs displayed increased anti-inflammatory potency. Phenotypic profiling of the cells in normal culture conditions demonstrated high levels of marker variability across donors, in addition to providing a reference for phenotypic comparison to MSCs derived from bone marrow, evidenced in the literature. Bone marrow is currently defined as the gold standard source of MSCs, and their similar phenotypic profile to C-MSCs found in this study authenticates the use of the cornea as a source for therapeutic cells. Furthermore, when compared to C-MSCs treated with inflammatory factors, makers both maintained, or demonstrating significant differences in levels of expression could be identified. The determination of C-MSC phenotype in an *in vitro* toxic microenvironment, presents a basis into understanding the different cellular pathways that would be activated if C-MSCs were administered to an injured cornea.

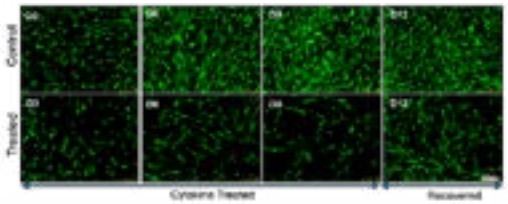

Fig.1: Effect of inflammatory stimuli on C-MSC viability, evidencing the live (green) and dead (red) cell populations.

DISCUSSION & CONCLUSIONS: Here we present initial steps into the use of C-MSCs as a cell therapy for ocular surface disorders, demonstrating increased secretion of anti-inflammatory factors from C-MSCs when treated with inflammatory agents, and identification of key similarities and changes in the phenotypic profile of the cells. These results provide an insight into the development of a C-MSC therapy with increased potency, and an understanding of the cell response to the injured ocular surface.

REFERENCES: 1. Morales, MLO., *et al., World journal of stem cells* 2019; 11:84.

3D bioprinting of conductive extracellular matrix structures towards cardiac tissue engineering

P. Sanjuan-Alberte[1,2], F. Ferreira[2], M. McAlpine[3], L.J. White[1], F.J. Rawson[1]

[1] *Regenerative Medicine and Cellular Therapies, School of Pharmacy, Biodsicovery Institute, University of Nottingham, University Park, Nottingham, NG7 2RD, UK*

[2] *Department of Bioengineering and Institute for Bioengineering and Biosciences, Instituto Superior Técnico, Universidade de Lisboa, Av. Rovisco Pais, Lisboa 1049-001, Portugal*

[3] *Department of Mechanical Engineering, University of Minnesota, Minneapolis, MN 55455, USA.*

INTRODUCTION: Conductive hydrogels are becoming increasingly popular, as smart- and stimuli-responsive materials could offer an additional degree of control over hydrogel properties and cell fate (1). Additionally, additive manufacturing methods can contribute towards controlling the overall shape and topography of hydrogels, representing a good alternative to commonly used casting methods (2). Development of conductive hydrogels compatible with 3D bioprinting can highly impact the field of cardiac tissue engineering by combining the biochemical features and tissue-like mechanical properties of the hydrogels with enhanced electrochemical properties.

METHODS: Decellularised extracellular matrix (dECM) hydrogels were printed using a 3D extrusion bioprinter and the freeform reversible embedding of suspended hydrogels (FRESH) method. Multiwalled carbon nanotubes (MWCNTs) were used as conductive nanofillers for the formulation of the dECM-based bioinks and combined with induced pluripotent stem cell-derived cardiomyocytes (iPSC-CMs).

RESULTS: dECM extracted from three different organs was used as the main component of our bioinks. These bioinks allowed for the 3D bioprinting of complex structures, demonstrating good printability (Figure 1). iPSC-CMs were incorporated into the bioinks and presented a viability >85% after the bioprinting process. Conductivity and mechanical properties enhancement of the materials was observed after incorporation of MWCNTs to the bioinks, with no detrimental effect to cell viability.

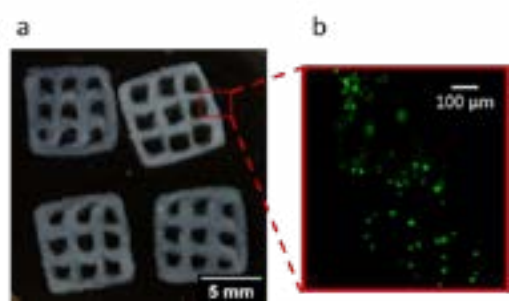

Fig. 1: (a) 10x10 mm dECM 3D printed scaffolds from bone decellularized tissue and (b) inset of fluorescence image of bioprinted iPSC-CMs after live/dead staining.

DISCUSSION & CONCLUSIONS: dECM-based conductive hydrogels were successfully 3D bioprinted in this work, supporting iPSC-CMs growth and viability

ACKNOWLEDGEMENTS: This work was supported by the Engineering and Physical Sciences Research Council (Grant numbers EP/R004072/1, EP/P027261/1 and EP/N006615/1) and an EPSRC Doctoral Prize award hosted by the University of Nottingham granted to Sanjuan-Alberte. J Jones and S Kellaway are acknowledged for their contribution in the tissue decellularization process.

REFERENCES:

(1) Distler, Thomas, et al. "Electrically Conductive and 3D-Printable Oxidized Alginate-Gelatin Polypyrrole: PSS Hydrogels for Tissue Engineering." *Advanced Healthcare Materials* (2021): 2001876.

(2) Sanjuan-Alberte, Paola, et al. "Development of Conductive Gelatine-Methacrylate Inks for Two-Photon Polymerisation." Polymers 13.7 (2021): 1038.

Low-pressure oxygen plasma treatment as a straightforward method for bioactivity enhancement *in-vitro* of a polyethylene terephthalate anterior cruciate ligament scaffold

T. Choreño Machain[1], S. Konan[1,2], U. Cheema[1]

[1] Centre for 3D models of Health and Disease, Division of Surgery & Interventional Science, University College London, London, GB, [2] University College Hospital NHS-Trust (UCLH), 235 Euston Rd, Bloomsbury, London, GB

INTRODUCTION: Anterior cruciate ligament (ACL) injuries represent 40% of all sports injuries in the United Kingdom (1). Since a complete rupture does not heal on its own, the treatment of choice is the reconstruction with a tendon autograft, leaving a second damaged site. A biocompatible synthetic graft could overcome this challenge. Short-time exposure to O_2 plasma was used to modify a polyethylene terephthalate (PET) scaffold aiming to improve the polymer's biocompatibility.

METHODS: PET 3D fibrous scaffolds were modified using a low-pressure plasma system operating at 40 kHz and 100 W, treating them with O_2 plasma for 0, 0.5 and 1 minute.

Biocompatibility was tested by seeding immortalized mesenchymal stem cells (iMSCs) onto the scaffolds and testing metabolic activity by means of a Presto Blue assay and DNA content using a Pico Green assay. Collagen deposition was assessed by staining with a Picrosirius Red dye, light microscopy imaging, and quantification of collagen after stain elution. DMEM-low glucose media supplemented with 50µg/mL ascorbic acid was used throughout all experiments. For all tests, seeded untreated PET scaffolds were used as positive control and unseeded PET scaffolds as negative control.

RESULTS: At day 7, the metabolic activity by cell number for the 1-minute O_2 plasma treated scaffold was significantly higher when compared to the 0.5 minute ($p=0.001$). From day 3 up to day 28, metabolic activity by cell number was higher ($p>0.9$) for the 1-minute treated scaffold. DNA content was higher for 1-minute O_2 plasma treated scaffolds from day 7 to day 28; only significantly different at day 21 when compared to the untreated scaffolds and at day 28 when compared to the 0.5-minute O_2 plasma exposed scaffolds.

iMSCs attached, proliferated, and effectively deposited collagen onto the fibrous scaffolds. Cells formed tri-dimensional colonies with cellular bridges from day 14. Total collagen production by DNA content was higher, although not significantly, at all three time points for the 0.5-minute treated scaffolds and for both plasma-modified scaffolds at days 14 and 28 ($p>0.08$) when compared to the untreated scaffold. There was no significant difference between 0.5 and 1-minute O_2 plasma treated scaffolds ($p>0.5$).

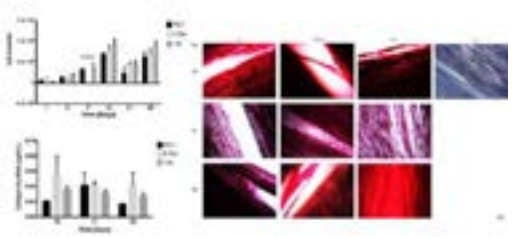

Fig. 1: Effect of O_2 plasma treatment on iMSCs proliferation and collagen deposition onto a PET scaffold. Bars represent the standard error of the mean ($n = 3$, $\alpha = 0.05$).

DISCUSSION & CONCLUSIONS: Low-pressure O_2 plasma treatment effectively modifies the hydrophobic and smooth PET surface. It offers a fast straight forward method for the surface modification of the PET ACL ligament scaffolds, supports cellular proliferation, and enhances collagen deposition. Additionally, the treatment could serve as an interfacial bonding layer for subsequent material adhesions to further increase the achieved bioactivity.

ACKNOWLEDGEMENTS: Work has been funded by the National Council of Science and Technology (CONACyT)-University College London (UCL) Graduate Fellowship.

REFERENCES: NHS. Hospital Accident and Emergency Activity - 2015-16 in Secondary Care Analysis ND. (ed. charts., E.t.a.).

Single-Administration Vaccine Enhancement (SAVE)

Kerr D.G. Samson[1], Veronica Hidalgo-Alvarez[1], Ferry P. W. Melchels[1]

[1] *Institute of Biological Chemistry, Biophysics and Bioengineering, School of Engineering and Physical Sciences, Heriot-Watt University. EH14 4AS Edinburgh, United Kingdom*

INTRODUCTION: The development of vaccines represents one of the most impactful milestones in the improvement of global health over the last 200 years[1]. As well as the administration of an antigen, vaccination requires the delivery of a booster which potentiates the immunostimulatory properties of the antigen[2]. Despite the undeniable success of vaccines, improvements in the delivery of these substances would be highly beneficial. The use of controlled release technology could circumvent the need for multiple injections in order to administer the booster doses. To achieve this, the present project aims to develop a single-administration vaccine (SAV) delivery device that is capable of delivering a booster at a specific time. This technology harnesses osmotic pressure as a trigger for the release of the booster, which is encapsulated in a polymeric capsule.

METHODS: Implantable capsules made of crosslinked poly (ε-caprolactone) (xPCL) were prepared by dip coating methacrylated PCL oligomers, followed by photocuring. Glucose was used as the osmotic agent and the food dye Brilliant blue FCF was employed to assess the osmosis-driven release kinetics. The devices were loaded with 70 µL of the glucose/dye stock solution and were incubated in PBS at 37 °C for 72 days in order to assess the dye release, which was quantified via UV spectrophotometry. The release from devices made of non-crosslinked PCL was evaluated for comparison. The cytotoxicity of the devices was evaluated by performing a WST-1 assay. Human dermal fibroblasts were seeded on disc-shaped polymer samples. Cell proliferation was assessed after 1, 4 and 11 days of culture.

RESULTS: The UV absorbance data obtained from the dye release studies showed that the burst delay time ranged between 25-30 days for xPCL. Devices made of PCL showed a gradual release that started at day 20 (Fig. 1). With regard to material toxicity, cells cultured on PCL and xPCL initially showed a reduced metabolic activity in comparison with the glass control group. However, the cell proliferation increased during the experiment (Fig. 2).

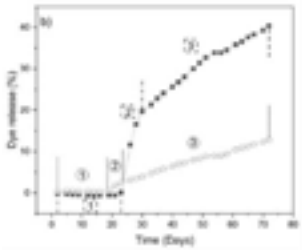

Fig. 1: Release profile of one representative capsule each of PCL (○) and xPCL (■).

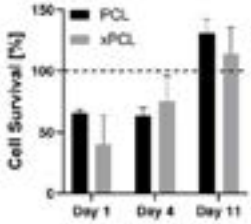

Fig. 2: Cell survival as measured via WST-1 assay. Data represents an average of triplicate samples ± SD. Reference line 100% indicates glass disc signal.

DISCUSSION & CONCLUSIONS: The results showed herein demonstrated the delayed burst release of a dye encapsulated in devices manufactured with a resorbable and non-cytotoxic polymer. The more elastic xPCL devices showed a burst release and, after 72 days of incubation, they had released 2-3 times more payload in comparison with PCL capsules.

ACKNOWLEDGEMENTS: The authors would like to thank BBSRC for providing financial support (*grant reference BB/R007616/1*).

REFERENCES:

1. Wallis, J. *et al*, Clinical & Experimental Immunology, 2019. **196**(2): p. 189-204.
2. Saroja et al., *Recent trends in vaccine delivery systems: A review.* International journal of pharmaceutical investigation, 2011. **1**(2): p. 64-74.

Manufacturing 3D co-cultures of the bone-tendon interface using human anatomical morphometrics

J.W. Mortimer[1], P.A. Rust[2], J.Z. Paxton[1]

[1] Anatomy@Edinburgh, Edinburgh Medical School: Biomedical Sciences, The University of Edinburgh, Edinburgh, EH8 9AG [2] Department of Plastic Surgery, Hooper Hand Unit, St John's Hospital, Livingston, Edinburgh, United Kingdom

INTRODUCTION: The bone-tendon interface (enthesis) is a complex anatomical junction that functions to transmit force smoothly between the soft tissues of tendon and the hard tissues of bone[1]. Injury to this region is common across the population, with a prevalence in young and active individuals. Surgical repair of the enthesis is poor and there is a clinical need to improve repair strategies [2]. Indeed, better 3D *in-vitro* models that mimic and re-establish the complex anatomy at this junction are required. This work aims to manufacture 3D co-culture *in vitro* bone-tendon constructs that are based on anatomical morphometrics specific to the flexor digitorum profundus tendon (FDPT) enthesis in the fingers.

METHODS: ***Anatomical morphometrics:*** Human cadaveric dissection was undertaken to establish overall characteristics of the human FDPT enthesis (size, shape and enthesis type; N=12 combined). ***Culture system design:*** Morphometrics were used to design a bespoke culture system to mimic FDPT anatomy and manufactured using 3D printing and PDMS molding. ***Human cell culture:*** Human osteoblasts and tendon fibroblasts were isolated from human surgical discard waste using established protocols and used to construct 3D co-culture constructs. ***3D co-culture:*** Bone portions were manufactured in brushite bone cement with specific anatomical dimensions and seeded with 15K human osteoblasts for 3 days before tendon formation. Tendon analogues were manufactured from fibrin scaffolds seeded with 200K human tendon fibroblasts. Co-cultures were maintained with 50:50 S-DMEM: Human Osteoblast Differentiation Medium at 37°C, 5% CO_2 for 14 days.

RESULTS: Anatomical morphometric analysis revealed a trapezoidal tendon insertion shape of mean surface area **29.29 ± 2.35 mm²** which, along with overall insertion dimensions, was used to manufacture brushite bone blocks. Also, angle of tendon insertion was measured histologically via digital imaging and calculated as **30.05 ± 0.72°** which, together with bone measurements, was used to design the bespoke culture wells (Fig 1A-B). 3D co-culture constructs began to form via fibroblast-mediated contraction and maintained a bone-tendon interface throughout the 14-day culture period (Fig 1C).

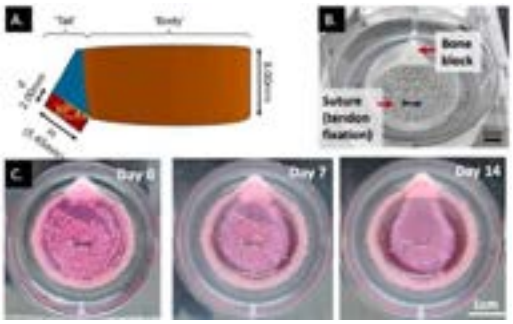

Fig. 1: A) CAD drawing of bespoke culture well design for FDPT enthesis constructs. B) Individual well with anatomically sized dimensions. C) 3D co-culture days 0,7,14, superior view

DISCUSSION & CONCLUSIONS: This study has shown that anatomically-relevant tissue-engineered constructs can be manufactured to specific anatomical dimensions and orthopaedic regions. Longer culture periods are currently under examination to assess overall gel contraction. Further work is needed to assess the mechanical and histological properties of the constructs and to compare to native tissue. Ultimately, this work aims to make bespoke constructs for implantation and improve clinical outcomes.

ACKNOWLEDGEMENTS: This work was funded by ORUK and The Rooney Plastic Surgery and Reconstructive Surgery Trust. Special thanks to those individuals who generously donated their body for research and education.

REFERENCES: 1. Apostolakos et al., (2014) Muscles Ligaments Tendons J. 17;4(3):333-42
2. Paxton et al., (2012) Orth Musc Sys S1

Towards scaffold-less bone production: investigating spheroid formation in rat osteoblasts

V. Prabhakaran[1], J.Z. Paxton[1]

[1]*Anatomy@Edinburgh, Edinburgh Medical School: Biomedical Sciences, University of Edinburgh, Scotland, UK*

INTRODUCTION: Three dimensional (3D) in-vitro spheroid cell cultures are cellular aggregates formed by self-assembling process that emulate in-vivo cell organisation [1]. There is limited information available on the use of spheroid culture for bone cells. We are particularly interested in the capacity for bone cells to form spheroids to develop a novel scaffold-free co-culture for musculoskeletal tissue interface formation. The aims of this study were (i) to identify the capacity of rat osteoblasts to form 3D spheroids by assessing cellular aggregation and (ii) establish a simple procedure for complete dissociation of spheroids for further molecular and biochemical analyses into cell function.

METHODS:

Spheroid formation: Differentiated rat osteoblasts (dRobs) [2] were cultured as monolayer in T75 flask in growth medium (DMEM supplemented with 10% fetal bovine serum and 1% antibiotic-antimycotic solution) at 37°C and 5% CO_2. These cells were dissociated and seeded at three different concentrations ($1x10^4$, $5x10^4$, $1x10^5$ cells/ 150 µl growth media) in 96 well cell repellent U bottom plate in triplicates and observed for spheroid formation under inverted microscope at different time points (12h, 24h, 36h and 48h). Spheroid diameter (n=3) was measured by ImageJ software.

Spheroid dissociation: dRobs ($5x10^4$ cells/150 µl growth media) were seeded in 96 well U bottom plate and allowed to form spheroids. After 24 hrs, the spheroids were maintained in rat osteoblast differentiation medium. The experiments were carried out on Day 1, 4, 7 after cell seeding in triplicates. First, the medium was removed, and the spheroids were washed twice with 100 µl 1X PBS. TrypLE Express (37°C) and Accutase (both 37°C and Room Temp.) were dissociation reagents tested. 50 µl of these reagents were added to each well and incubated at respective temperatures for different time periods ranging from 4 to 50 minutes. After incubation, spheroids were disaggregated by pipetting followed by addition of 150 µl media to arrest the reagent action. Cell count and viability (trypan blue) assays were performed using haemocytometer (n=3).

RESULTS: Spheroid formation: Osteoblasts at all three concentrations were fully aggregated at 24h after which the spheroids constricted to form compact structures (Fig 1). **Spheroid dissociation**: Accutase (30 mins @ 37°C) resulted in complete disaggregation into single cell suspension with >90% viability.

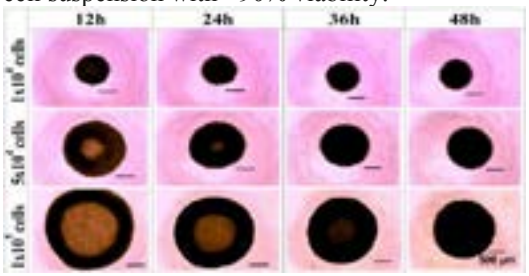

Fig. 1: Spheroid formation of different cell concentrations at different time points

DISCUSSION & CONCLUSIONS: The time taken for rat osteoblasts to form a full spheroid aggregate is 24 h, similar to other studies [3]. The spheroid size gradually decreased with time in the initial period due to tight aggregation and reduction in cell diameter [4]. Spheroids can be effectively dissociated into single cells by accutase (30 minutes at 37°C). This is a crucial step for future studies that will focus on the molecular and biochemical behaviour of rat osteoblasts in spheroid monoculture and co-culture with other musculoskeletal cell types.

ACKNOWLEDGEMENTS: VP is funded by the Principal's Career Development Award and the Edinburgh Global Research Scholarship, University of Edinburgh.

REFERENCES:

1. DuRaine, G. D. et al. (2015), Annals of Biomedical Engineering, 43(3). 2. Alsaykhan, H.M. (2019), PhD thesis, University of Edinburgh 3. Zhang, M. et al. (2020) Biomaterials, 260. 4. Grässer, U. et al. (2018) Annals of Anatomy, 216.

Additive Manufacture of Vascularised Hybrid Scaffolds for Bone Tissue Engineering

NRE. Putri[1,2], R. Wildman[1], F. Rose[3], L. Ruiz -Cantu[1]

[1]*Centre for Additive Manufacturing, Faculty of Engineering, University of Nottingham*

[2] *Department of Chemical Engineering, Faculty of Engineering, Universitas Gadjah Mada*

[3]*Biodiscovery Institute, School of Pharmacy, University of Nottingham*

INTRODUCTION: One of the main limitations in engineering in vitro tissues is the lack of a sufficient blood vessel system, leading to cell death due to nutrient and oxygen shortage. Several methods have been developed to fabricate capillaries within scaffolds before implantation. However, replicating the complex architecture of vascular channel and functionality of the capillary is still challenging. Additive manufacturing or 3D printing is a technology that can be used to create complex architectures and control the composition of scaffolds.

Natural polymers such as gelatin methacrylate (GelMA) have been previously explored in 3D printing technology for regenerative medicine applications. It has excellent biocompatibility, good cell adhesion properties, and high water solubility[1,2]. However, GelMA has poor mechanical properties and fast degradation *in vivo*. Therefore, the addition of synthetic polymer into the GelMA ink can be conducted to solve those limitations. Poly trimethylene carbonate (PTMC) which has adjustable mechanical properties and non-acidic degradation products[3] can be used as a blend.

This work aims to fabricate vascularized scaffold using inkjet 3D printing and biodegradable hybrid materials such as GelMA and PTMC.

METHODS: The amphiphilic PTMC-PEG-PTMC tri block co-polymer was synthesized and diacrylated following Ruiz et al[4]. Different concentrations of GelMA and the co-polymer were explored to obtain the optimum ink composition. Biocompatibility studies of the formulation were performed using immortalized human mesenchymal stem cells. A commercial water soluble (WS) ink was used as fugitive ink to form the vascular channel using multi-material inkjet printing.

RESULTS: The synthesized diacrylated PTMC-PEG-PTMC copolymer was a viscous liquid at room temperature and had a wax consistency at temperatures lower than 4 °C. The blend solutions of copolymer and GelMA formed a homogeneous solution with the optimum composition of 1.5 wt.%, 10 wt.%, and 5 wt.% in water and DMSO solution for GelMA, copolymer, and PEGDA, respectively. Biocompatibility studies showed not toxicity and good cell adhesion to the material. On the microchannels printing studies we obtained droplet sizes of 68 µm with the WS ink, which allowed the fabrication of small vascular channels (75 µm diameter). The inkjet 3D printed microchannels are shown in Fig. 1.

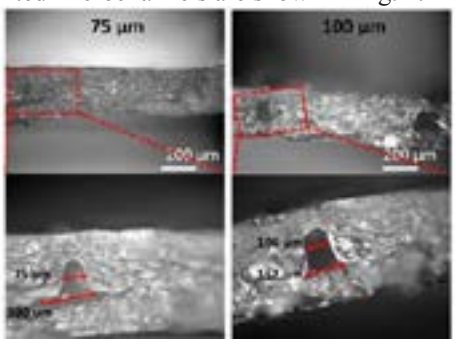

Fig. 1: Inkjet 3D printed microchannels with 75 µm and 100 µm diameter.

DISCUSSION & CONCLUSIONS: A biocompatible hybrid hydrogel bioink was successfully prepared. In this study it was also demonstrated is possible to create micro channels with the same dimensions than capillaries using multi material inkjet printing. Future studies will involve the fabrication of a clinically relevant size scaffolds with integrated vasculature.

REFERENCES:

[1] [Liu], [Y.] and [Chan-park], [M.B.], Biomat., 31(6):1158-1170, 2010.
[2] [Nichol], [J.W.] *et al*., Biomat., 31:5536-5544, 2010.
[3] [Fukushima], [K], Biomat. Sci., 4:9-24, 2016.
[4] Ruiz-Cantu et al., ChemRvix 2020

Microfluidic Development of Microparticles to Enhance Cell Engraftment

K.Patel[1,2,3], AA.Dundas[1,2], I.Lee[1,3], R.Wildman[1,2], DJ.Irvine[2], LJ.White[1,3]

[1]School of Pharmacy, University of Nottingham, GB, [2]Centre for Additive Manufacturing, University of Nottingham, GB, [3]Biodiscovery Institute, University of Nottingham, GB

INTRODUCTION: Intrahepatic engraftment of islets or hepatocytes can eliminate the need for pancreas or liver transplantation. But, poor revascularisation and inflammatory reactions results in approximately 60-70% of cells failing to engraft. The delivery of immunomodulatory molecules such cytokine inhibitors, and growth factors including cytokines, has been shown to increase cell engraftment. However, delivering and maintaining these molecules locally at therapeutic doses remains a significant challenge. We propose a new paradigm of PLGA-based microparticles fabricated using microfluidic droplet methods as a replicable, automated, and scalable process to produce highly monodispersed microparticles that can provide a tuneable and controlled release. The inclusion of galactose will enable binding to hepatocytes in the liver(1) to ensure localised delivery of immunomodulatory molecules.

METHODS: Poly(D,L-Lactide-co-Glycolide) (PLGA) 50:50, Mw 61kDa, and galactosylated PLGA (Gal-PLGA), synthesised using D-(+)-Galactose Mw 180Da chemically attached to PLGA, microparticles were fabricated using a 100µm flow focusing hydrophilic microfluidic chip. PLGA and Gal-PLGA were dissolved in Dichloromethane (DCM) Mw 85Da, to form the dispersed phase. A surfactant solution of Poly(vinyl alcohol-co-vinyl acetate) (PVA) 88% hydrolysed, Mw 25kDa, in deionised water made the continuous phase. A syringe pump was used to push both the dispersed and continuous phases through the chip at a rate of 0.15ml/hr and 4ml/hr respectively. At the junction where the dispersed and continuous phase met, droplets pinched off and were collected in deionised water.

RESULTS: 10% PLGA with 2% PVA in water was used with microfluidics (*Fig. 1*).

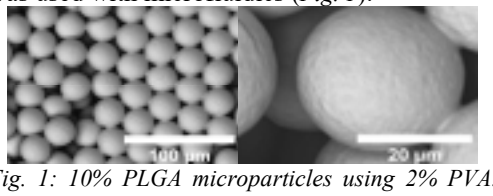

Fig. 1: 10% PLGA microparticles using 2% PVA. X800 magnification (left), and X4000 magnification (right).

Table 1. Microparticles fabricated using 10% PLGA with varying PVA concentrations. Shows average particle diameter, and resultant polydispersity index (PDI) and coefficient of variance (CoV) values.

PVA (w/v)	Average Diameter (µm)	PDI	CoV %
2%	23.52	0.0071	8.42
1%	26.11	0.00086	2.93
0.5%	30.74	0.031	17.73

Microfluidics produced particles with low polydispersity (*Table 1).* The reduction in PVA concentration caused an increase in the average particle size. Furthermore, low system stability was observed when 0.5% PVA was used. Lastly, 7% Gal-PLGA was used with 2% PVA. However, notable pores were observed therefore the concentration of PVA was decreased to 1% PVA which reduced the extent of porosity but did not eliminate it (*Fig. 2).*

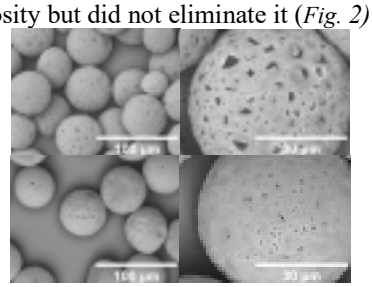

Fig. 2: 7% Gal-PLGA microparticles using 2% PVA (top row) and 1% PVA (bottom row). Both at X800 magnification (left), X3000 magnification (right).

DISCUSSION & CONCLUSIONS: Microfluidics has the potential to produce monodispersed microparticles. To achieve this, optimisations of materials, surfactants, and operations are needed. Gal-PLGA can also be used as a material to form microparticles. However, it is also evident that further material characterisation is needed to eliminate porosity.

ACKNOWLEDGEMENTS: Funded by UKRMP, BBSRC, EPSRC, and MRC.

REFERENCES:

1. D'Souza AA, Devarajan PV. Asialoglycoprotein receptor mediated hepatocyte targeting-strategies and applications. J Control Release. 2015;203:126-39.

MODIFYING BONE SCAFFOLD CHARACTERISTICS IN AN ANATOMICAL INTERFACIAL TISSUE ENGINEERED MODEL

C. Loukopoulou[1], J.W. Mortimer[1], P.A. Rust [2], J.B. Vorstius [3], J.Z. Paxton[1]

[1]Edinburgh Medical School: Biomedical Sciences, The University of Edinburgh, EH8 9AG, Edinburgh
[2] Hooper Hand Unit, NHS Lothian, St John's Hospital, EH54 6PP, Livingston [3]Fulton Building, School of Science and Engineering, University of Dundee, DD1 4HN, Dundee.

INTRODUCTION: A subdiscipline of Tissue Engineering, interfacial TE (ITE), is particularly aimed at reconstructing the enthesis, the specialised transition zone between soft tissue and bone allowing for smooth force transmission.

One of our group's main research areas is the study of avulsion injury of the flexor digitorum profundus (FDP) tendon at its insertion onto the base of the distal phalanx in the hand. Recent work has focused on improving an existing *in vitro* tendon-bone model, where a tendon equivalent is formed by contraction of cell-seeded fibrin and is directed to attach to a custom-made bone anchor. Further work exhibited specific dimensions of the FDP insertion footprint which guided the design of our bone anchors.

Latest advances in materials science have enabled the production of scaffolds that more effectively mimic the hierarchical features of bone matrix. By modifying the presenting surface of the bone anchor and introducing a more hierarchical structure, we will evaluate changes in fibrin gel attachment and osteoblast adhesion and proliferation.

METHODS: Human cadaveric dissection was employed to expose the anatomy of the FDP footprint and interface angle which were later analysed using ImageJ. Obtained anatomical morphometrics guided the Tinkercad (©2021 Autodesk, Inc.) CAD design of various molds for bone anchors, which were later 3D printed in Acrylonitrile Butadiene Styrene (ABS). Molds were used to produce negative silicone impressions to create custom-made bone anchor in our material of choice, brushite ($CaHPO_4 \cdot 2H_2O$) cement. Different surface patterns were developed in prospect of increasing the surface area (SA) of the bone anchor where it is in direct contact with the tendon analogue.

RESULTS: The aforementioned methodology revealed a trapezoidal-shaped FDP footprint with mean anatomical measurements for all fingers combined ('universal' size) were 6.47mm±0.21mm (height), 8.58mm±0.37mm (base width), and 1.60mm±0.11mm (apex width). These measurements were used to construct a 'plain' bone anchor mold design (Fig 1A) and subsequent brushite bone block of exact anatomical dimensions (Fig 1B) To increase surface area of the presenting bone anchor surface, additional designs were created with modified surface patterns including grooves, gridlines, posts and pits (Fig.2).

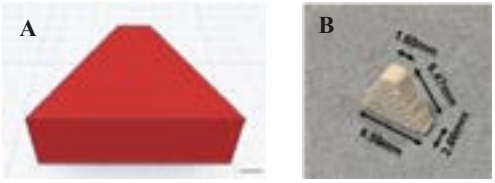

Fig 1: **A**) Original bone anchor design made with Tinkercad (©2021 Autodesk, Inc) based on existing anatomical morphometrics. Scale bar 8.6mm. **B**) Brushite bone anchor in 'Universal' size with anatomical dimensions.

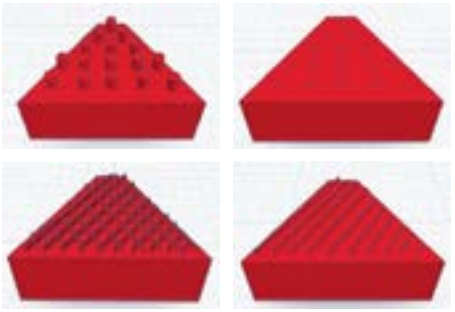

Fig 2: Different surface patterns to increase SA. Designs made with Tinkercad (©2021 Autodesk, Inc) based on existing anatomical morphometrics. Top left: 1mm posts; top right: 1mm pits; Bottom left&right: multiple and single gridlines respectively.

DISCUSSION & CONCLUSION: The new mold designs will be used to manufacture brushite cement bone anchors and substitute the 'plain' bone anchor in our *in vitro* tendon-bone model to evaluate their efficacy in a co-culture system. There is also potential to assess fibrin gel attachment via mechanical testing. Ultimately, we propose that by modifying the presenting surface of our bone anchors, we will encourage osteoblast adhesion and proliferation and improve fibrin gel attachment in our ITE model.

ACKNOWLEDGEMENTS: Our special appreciation to the body donors and Edinburgh Medical School. Funding kindly provided by Orthopaedic Research UK (projects 528 and 533).

Serum-free Osteogenic Differentiation of Mesenchymal Stem Cell Line

J. Rodrigues[1], D. Syla[1], G. Reilly[1], F. Claeyssens[2]

[1]Univ Sheffield, INSIGNEO Inst Silico Med, Sheffield, S Yorkshire, England, [2]Univ Sheffield, Kroto Res Inst, Dept Mat Sci & Engn, Sheffield, S Yorkshire, England

INTRODUCTION: Variability can be a major issue for *in-vitro* biological testing. One of the main sources of variability can be the culture media used, generally supplemented with animal serum. Foetal Bovine Serum (FBS) from different sources, for example, was shown to affect differently the osteogenic differentiation of Mesenchymal Stem Cells (MSCs) [1]. Serum-free alternatives, with controlled compositions, can mitigate variability in results. However, for cells with heterogeneous populations like MSCs, it can be difficult to find a good serum-free alternative. This work aims to compare a commercially available serum-free media to different serum-containing media, for the osteogenic differentiation of an immortalized MSC cell line.

METHODS: A MSC cell line immortalized with the human telomerase gene (hTERT-MSC Y201[2]) was cultured for 21 days (timepoints at day 7, day 14, and day 21) in three different media, with and without osteogenic supplementation, and with different media change protocols (1 full change a week, 3 half changes a week, 3 full changes a week). Table 1 details the composition of each media.

Table 1 - Media composition

Media	Composition
BM3	DMEM (GIBCO) + 10% FBS (GIBCO)
CD1	StemMACS™ MSC Expansion Media Kit XF, human (Miltenyi Biotec), serum-free and xeno-free
HSM	Human Mesenchymal-XF Expansion Medium (Merck), human-serum

L-Ascorbic Acid 2-phosphate (AA2P), beta-glycerophosphate (βGP) and dexamethasone (DEX) were used to induce osteogenesis. Two different supplementation profiles were used: OM1, where AA2P was added on day 2 and βGP and DEX at day 5; OM2, where all supplements were added at day 2. For each condition at each timepoint it will be measured cell metabolic activity by resazurin reduction assay, alkaline phosphatase activity by colorimetry, calcium deposition by Alizarin Red S staining, and collagen synthesis by Sirius Red staining.

RESULTS: Early results show that cell metabolic activity in CD1 is generally comparable to that of BM3 and HSM, regardless of media change protocol. Moreover, the addition of osteogenic supplementation, does not have a negative impact on metabolic activity, nor does the different media change protocols. Optical microscopy suggests that, for all media, 1 full media change following the OM2 supplementation profile provides the best results. CD1 (figure 1) seems to have perform better in this regard compared to BM3 and HSM.

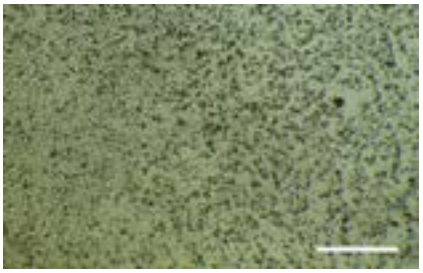

Figure 1 – Day 21 of Y201 cells in CD1, 1 full media change a week, following OM2 supplementation protocol. Scale bar = 500 µm.

DISCUSSION & CONCLUSIONS: Current results suggest that CD1 can outperform both BM3 and HSM for the osteogenic mineralization of hTERT-MSCs Y201. Regardless of media, 1 full media change a week following the supplementation profile OM2 seems to provide the best results. Future work will help corroborate these findings, as well as indicate how collagen synthesis is affected. Overall, it is shown that serum-free media can be an effective alternative to serum-containing media for hTERT-MSCs Y201.

ACKNOWLEDGEMENTS: This project has received funding from the European Union's Horizon 2020 research and innovation programme under the Marie Skłodowska-Curie grant agreement No 766012.

REFERENCES: [1] J. Melke, Eindhoven University of Technology, 2019. [2] S. James, *et al.*, Stem Cell Reports 4(6) (2015) 1004-1015.

Novel formulations for the spray delivery of therapeutic cells for traumatic brain injury

A. Nash[1], S. Broccini[2], J. Phillips[2], L. White[1] , and M. Marlow[1]
[1]*Universiy of Nottingham,* [2] *University College London*

INTRODUCTION: Current therapies for traumatic brain injury (TBI) aim to limit further damage occurring as a response to the initial trauma. Animal studies have shown improved neurological outcomes following mesenchymal stem cell (MSC) transplant (1), however successful delivery of these cells is limited by the delivery route. We hypothesise that delivering these cells locally by spraying within a hydrogel-forming pectin solution will enhance recovery outcomes.

METHODS: Cell spraying was assessed using 3T3 mouse fibroblasts. Cell suspensions were prepared at varying cell densities and used to seed plates by spraying or syringing the cells. Cell viability was assessed using an alamarBlue assay.

The cytotoxicity of 2 different grades of pectin with different degrees of esterification, both before and after undergoing an activated charcoal purification protocol, were assessed using a human immortalised MSC line. Cell culture media was conditioned with pectin gels at 37 °C for 24 hours before being added to cells in culture. Pectin gels were also added directly onto cells in culture. Cell viability was assessed using a prestoBlue assay.

RESULTS:

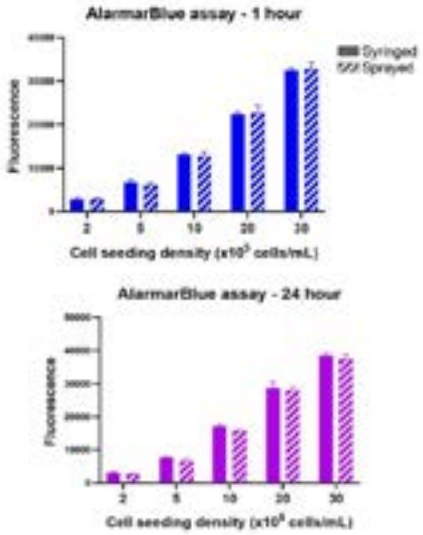

Fig. 1: Effect of spraying on 3T3 mouse fibroblast cells. Cell viability was assessed 1 hour, and 24 hours following spraying and compared to cells seeded using a syringe.

Metabolic activity of 3T3 mouse fibroblasts was not affected by spraying or cell density.

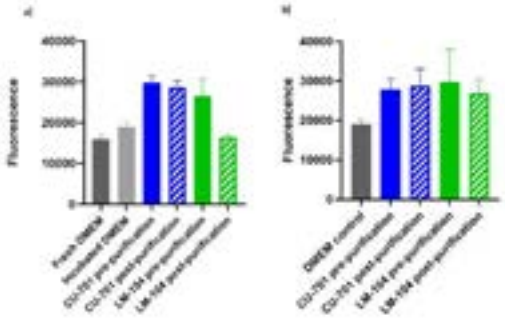

Fig. 2: Effect of a) pectin conditioned media, and b) pectin gels on human immortalised MSC viability.

The metabolic activity of the cells increased following the addition of media conditioned with CU-701 grade pectin and the not purified LM-104 grade pectin. The metabolic activity of the cells increased in all instances where pectin gels were placed in culture with the cells.

DISCUSSION & CONCLUSIONS: 3T3 mouse fibroblasts survived the process of spraying, however they are well known to be a robust cell line, therefore this experiment will be repeated with human MSCs.
Human immortalised MSCs did not decrease in metabolic activity, suggesting pectin is not cytotoxic. An increase in metabolic activity was observed in most conditions therefore further investigation is required to understand the reason for this.

ACKNOWLEDGEMENTS: Funded by the EPSRC (EP/L01646X/1). CDT in Advanced Therapeutics and Nanomedicine.

REFERENCES:
(1) Adult Bone Marrow Stromal Cells Administered Intravenously to Rats after Traumatic Brain Injury Migrate into Brain and Improve Neurological Outcome. Lu, Dunyue, et al. s.l. : NeuroReport, 2001, Vol. 12.

Expansion of Human Mesenchymal Stem Cells under Serum-Free Conditions

D. Syla[1], J. Rodrigues[1], G. Reilly[1], F. Claeyssens[2]

[1]Univ Sheffield, INSIGNEO Inst Silico Med, Sheffield, S Yorkshire, England, [2]Univ Sheffield, Kroto Res Inst, Dept Mat Sci & Engn, Sheffield, S Yorkshire, England

INTRODUCTION:

The lack of uniformity in sera compositions leads to variable and inconsistent in-vitro cell behaviour by altering overall cell metabolism. Serum-free media can provide a more consistent performance and avoid masking of biological tests. The replacement of serum and adaption of conditions requires the understanding of the individual cell behaviour. In this project we aim to test cell expansion with serum and serum-free media to analyse optimal conditions for fast cell expansion.

METHODS: The used cell line is a Mesenchymal Stem Cell (MSC) line immortalized with the human telomerase gene (hTERT-MSC Y201. Cells were seeded in a density of 4000 cells/cm2 in well-plates that were non-coated, coated with fibronectin and coated with gelatin. Cells were cultured for 7 days with 3 different media (1 with serum, 2 without serum) and no media changes, 1x full media change and 1x partial media change.

Table 1 Media types used and composition

Media	Composition
BM3	DMEM (GIBCO) + 10% FBS (GIBCO)
CD1	StemMACS™ MSC Expansion Media Kit XF, human (Miltenyi Biotec), serum-free and xeno-free
HSM	Human Mesenchymal-XF Expansion Medium (Merck), human-serum

Each media was tested with different coatings and media changes (media x coating x media change) for time points on day 1, day 4 and day 7 by measuring metabolic activity by resazurin reduction assay and DNA assay.

RESULTS:

The results showed that all media provided high cell metabolism. We could see that CD1 had the highest cell metabolism in all media types and showed the best results when coated with fibronectin or gelatin and without any media changes.

Table 2 Resazurin on Day 7

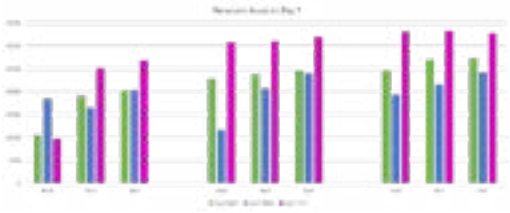

DISCUSSION & CONCLUSIONS: Results show that the use of CD1 has the best results when used together with a coating and not treated with any media changes.

ACKNOWLEDGEMENTS: This project has received funding from the European Union's Horizon 2020 research and innovation programme under the Marie Skłodowska-Curie grant agreement No 766012

Using Nanoscale Mechanotransduction to Stimulate Differentiation of Neural Stem Cells and Glioblastoma- Derived Cancer Stem Cells

S.R.Dallas[1], S.Smith [1], P.M. Brennan [2]

[1] Institute for Bioengineering, School of Engineering, The University of Edinburgh, SMC, Alexander Crum Brown Road, EH9 3JF, Edinburgh [2] Centre for Clinical Brain Sciences, The University of Edinburgh, 49 Little France Crescent, EH16 4SB, Edinburgh

INTRODUCTION: Stem cells are found in various niches within the human body, including the central nervous system, the gut and bone marrow[1]. Cancer stem cells have been found in varying amounts inside Glioblastoma Multiforme (GBM) tumours[2]. The specific sites at which the cell is in contact with the extracellular matrix (ECM) are known as focal adhesions, and there are many proteins which function at this site, thus allowing the cell to respond to mechanical cues from its external environment[3,4]. Using a device called a 'Nanokicker,' controlled nanoscale vibrations can be administered to the cells- this technique has already been used to stimulate the differentiation of Mesenchymal Stem Cells into osteoblasts[5].

METHODS: Cells were exposed to differentiation stimulation by nanoscale mechanotransduction (NM) or a chemical stimulation: Bone Morphogenic Protein 4 (BMP4). The media also contained Epidermal Growth Factor (EGF) and Fibroblast Growth Factor-2 (FGF). Experiments were carried out with and without the inclusion of these growth factors (GF). After 7 days, changes in gene expression were measured against a control group using qPCR.

RESULTS: Results show an increase in Glial Fibrillary Acidic Protein (GFAP) expression when GF are removed from the cell culture media. Small increase in GFAP expression with addition of BMP4 in presence of GF.

DISCUSSION & CONCLUSIONS: GFAP expression is associated with astrocytic differentiation. The removal of GF has the biggest impact on stem cell differentiation, while cells grown in media containing BMP4 and GF did show a small increase in differentiation. GF in the media greatly reduced differentiation.

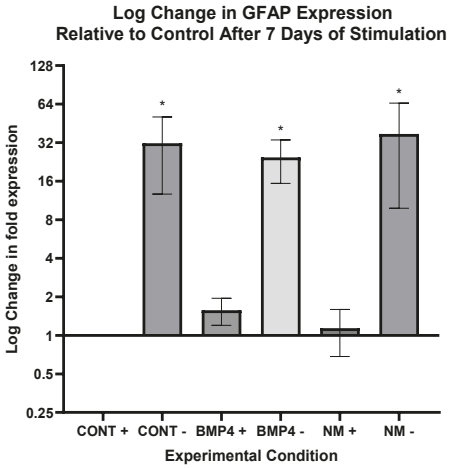

Fig.1 GBM Cells stimulated with BMP4 or NM, with (+) or without (-) the addition of growth factors. Error bars show SD.

ACKNOWLEDGEMENTS: M. Dalby, S.Reid, M. Hughes, P. Brennan, M. Shipston, J. Paxton

REFERENCES:

1. Ferraro, F., Celso, C. L. & Scadden, D. Adult Stem Cells and Their Niches. Adv. Exp. Med. Biol. 695, 155–168 (2010).

2. Quintana, E. et al. Efficient tumor formation by single human melanoma cells. Nature 456, 593–598 (2008).

3. Kanchanawong, P. et al. Nanoscale architecture of integrin-based cell adhesions. Nature 468, 580–584 (2010).

4. Bershadsky, A. D., Balaban, N. Q. & Geiger, B. Adhesion-Dependent Cell Mechanosensitivity. Annu. Rev. Cell Dev. Biol. 19, 677–695 (2003).

5. Nikukar, H. et al. Osteogenesis of Mesenchymal Stem Cells by Nanoscale Mechanotransduction. ACS Nano 7, 2758–2767 (2013).

Studying the Localisation of Nuclear Lamina Proteins in Human Pluripotent Stem Cell-derived Motor Neurons

Author: Divine Adegbie

Supervisor: Dr. Francesco Saverio Tedesco, Co-Supervisor: Mr Luca Pinton

Cell and Developmental Biology Lab, University College London, London, GB

INTRODUCTION: Lamins are type V intermediate filament proteins essential for maintaining nuclear integrity and cell viability. They have been implicated in various diseases termed 'laminopathies', some of which can also affect the nervous system. Laminopathies are a group of diseases caused by mutations in lamin genes, particularly LMNA; at least 13 diseases have been linked to LMNA mutations [1]. Mutations in LMNA lead to chromosome aneuploidy, chromosomal breaks, nuclear blebbing, abnormal clustering of NPCs, loss of lamins at the periphery and a honeycomb-like appearance of the lamina which can be observed in the abnormal nuclear morphology of disease cells.

METHODS: To model CMD, skeletal muscle precursors, derived from healthy donors and patient-derived LMNA-mutant iPSCs, will be first expanded and then directed via the mesodermal lineage to become skeletal muscle, forming myotubes according to an already established protocol[2]. They will act as controls for lamin localisation dynamics and nuclear abnormalities. The control lines are necessary for comparison and standardisation of the experiment. Expression of lamin-A/C and lamin-B1 in these cells will be compared to expression in a healthy motor neuron after neural precursors are expanded and directed via the ectodermal lineage to become motoneurons according to an unpublished adapted protocol by the Patani Lab at UCL[3]. These cell lines will be fixed and stained using immunostaining techniques to observe their nuclear morphology for any abnormalities and mis-localisations of lamin-A/C, and lamin-B1.

RESULTS: Evidence indicates that the mis-localisation of Lamin-B1 can result in the appearance of capping and honeycomb-like nuclear structures. Observation of the images captured showed that LMNA-mutant myotubes had a significantly higher percentage occurrence of Lamin-B1 mis-localisation (capping) at 2.83 %, almost 7x higher than the percentage found in motor neurons (0.39%).No significant difference was found between motor neurons and healthy control myotubes. A significant difference was found between motor neurons and *LMNA*-mutant myotubes.The presence of abnormally-shaped nuclei is a characteristic cellular phenotype of laminopathies. Circularity analyses showed no significant differences between the LMNA-mutant myotubes, the healthy myotube control and motor neuron lines.

Fig. 1: Experimental lines immunostained for Lamin-B1.

- **DISCUSSION & CONCLUSIONS: This project has shown that healthy motor neurons do not show the nuclear abnormalities characteristic of laminopathy lines.**
- **They exhibit a phenotype similar to the normal control myotube nuclei and dissimilar to the LMNA-mutant myotube nuclei, with a relatively low percentage of capping, blebbing and other nuclear abnormalities.**
- **They therefore can be used as reliable controls in further disease modelling studies for Charcot-Marie-Tooth laminopathies.**

ACKNOWLEDGEMENTS: Dr. **Francesco Saverio Tedesco, Luca Pinton,** Heather Steele-Stallard, Dr. Shilpita Sarcar, Alexander Henderson, Dr. Louise Moyle, Dr. Giulia Ferrari, Moustafa Khedr, Past members: Dr. Sara Benedetti, Dr. Sara Maffioletti

REFERENCES:

- **[1] Capell and Collins, 2006**
  [2]Maffioletti et al 2015
  [3]Chen et al, 2014

A neurovascular 3D cell model to investigate the role of pericytes in dementia

M. Polleres[1], G. Potjewyd[1], T. Wang[1], M. Domingos[2,3], N. M. Hooper[1]

[1]Faculty of Biology, Medicine and Health, The University of Manchester, UK, [2]Faculty of Science and Engineering, The University of Manchester, UK, [3]The Henry Royce Institute, Manchester, UK

INTRODUCTION: Pericytes, brain micro-vascular endothelial cells (BMECs), astrocytes, and neurons form the neurovascular unit (NVU). Dysfunction of the NVU is commonly seen in vascular dementia and Alzheimer's disease (1). Pericytes have been shown to contract capillaries and thus reduce cerebral blood flow, in a downstream response to amyloid-β, a hallmark protein of Alzheimer's disease (2). However, the full role of pericytes in health and disease remain poorly understood, partially due to a lack of adequate models that can recapitulate the complexity of the multi-cellular NVU. The aim of this study is to incorporate pericytes into a 3D in vitro model to study the function, and dysfunction, of the NVU and the pericytes within it.

METHODS: Brain pericyte-like cells and BMECs were differentiated from human induced pluripotent stem cells (iPSCs; 3, 4) and co-cultured in a transwell-type NVU model. Integrity of the endothelial barrier function was evaluated by transendothelial electrical resistance (TEER) measurements. Hydrogel encapsulation was used as a contraction indicator.

RESULTS: Brain pericyte-like cells stained positively for pericyte markers NG2, PDGFR-β, CD13, and CD146. Co-culture of pericyte-like cells with BMECs resulted in a significantly increased TEER compared with mono-cultured BMECs. Furthermore, these brain pericyte-like cells significantly decreased the hydrogel surface area by 40% showing their potential ability to contract.

DISCUSSION & CONCLUSIONS: These results suggest that functional brain pericyte-like cells were obtained and can be incorporated into a NVU model. We will build on these findings to develop a robust model to study pericytes within the NVU to investigate their function and dysfunction in health and disease.

ACKNOWLEDGEMENTS: This study is supported by the EPSRC/MRC Centre for Doctoral Training in Regenerative Medicine (EP/L014904/1).

REFERENCES:

1. Kisler K, Nelson AR, Montagne A, Zlokovic BV Nat Rev Neurosci. 2017; 18; 7.

2. Nortley R, et al. Science 2019; 365; 6450.

3. Stebbins MJ, et al. Methods. 2016; 101.

4. Faal T, et al. Stem Cell Reports. 2019; 12; 3.

Topographically Featured PCL Electrospun Scaffolds Incorporating Rat Liver Extracellular Matrix (ECM) for Liver Tissue Engineering

Yunxi Gao, Anthony Callanan
Institute of Bioengineering, School of Engineering, The University of Edinburgh, Edinburgh, United Kingdom

INTRODUCTION: Electrospun polymer scaffolds provide a biomimetic microenvironment and mechanical support for tissue regeneration[1]. The morphology of scaffolds and biological additives have been shown to have significant effects on cell behaviour[2,3]. In this study, we investigated the incorporation of decellularized liver ECM into topographically featured PCL fibres to produce a novel ECM-PCL scaffold for hepatocyte culture and tested the response of Hepg2 cells.

METHODS: Whole rat liver was harvested from mature male Sprague-Dawley rat, then it was decellularized by 0.25w/v% Sodium Dodecyl Sulphate (SDS) solution and ultra-pure water. Decellularized liver was then cut and digested in 1% pepsin solution for 72 hours. After freeze-drying, the ECM was homogenized and blended with PCL pellets in different solvent systems. 0.07% ECM, 0.14% ECM, depression only and no depression scaffolds were eventually fabricated. HepG2 cells were seeded onto these scaffolds for up to 14 days, cell viability, DNA content, albumin secretion, gene expression, immunostaining were conducted at 24 hours, 7 and 14 days.

RESULTS: We successfully fabricated four different consistent scaffolds with similar fibre diameter (4um). A cell monolayer produced on both ECM scaffolds on day 14, while more cell spreading showed on the other scaffolds without ECM (Fig.1). The results show higher cell viability in the scaffold without ECM (Fig.2). All scaffolds maintained the same albumin secretion, and 0.14% ECM scaffold shows the highest albumin level. Gene expression also shows higher fibronectin production on 0.14% ECM scaffold.

DISCUSSION & CONCLUSIONS:
In this study, we successfully combined ECM and electrospun topographical tailored fibre scaffold. Cellular testing revealed HepG2s reacted to the addition of a small amount of ECM and showed different cellular responses at all time points. The ECM-PCL scaffold can maintain the liver typical gene expression while the cells grow more on the scaffold without ECM. These results therefore provide evidence on the modification potential of fibre scaffolds for liver tissue engineering.

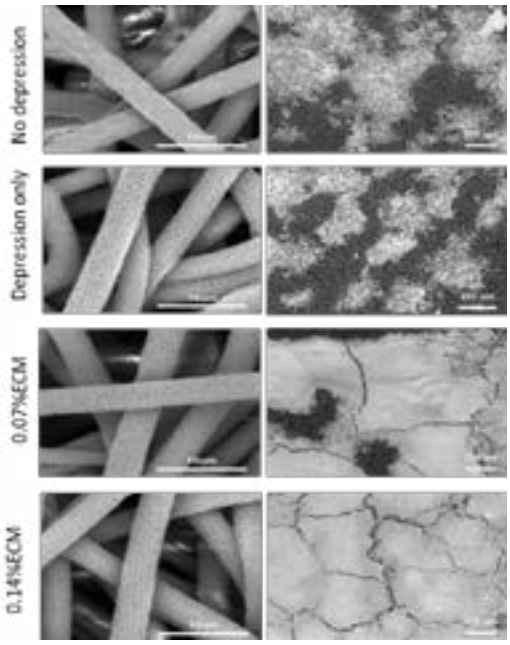

Fig. 1: Fibre morphology and cell distribution at 14 days.

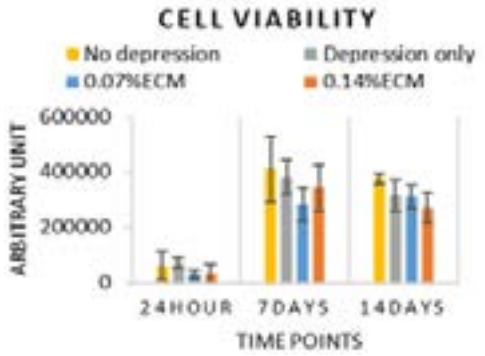

Fig.2: Cell viability at all time points.

ACKNOWLEDGEMENTS: MRC grant MR/L012766/1.

REFERENCES:
1. Grant R et al. Sci Rep. 2019 Dec 1;9(1).
2.Reid JA, Callanan A. J Appl Polym Sci. 2019;48181:48181.
3. Bate TSR et al. Sci Rep [Internet]. 2021;11(1):1–13. Available from: https://doi.org/10.1038/s41598-021-81761-z.

Engineering Osteochondral Tissue Gradients

J. P. K. Armstrong[1], C. Li[1], L. Ouyang[1], M. M. Stevens[1]

[1] *Department of Materials, Department of Bioengineering, and Institute of Biomedical Engineering, Imperial College London, England, GB.*

INTRODUCTION: Gradients are an important feature of many natural tissues [1]. A classic example is the osteochondral interface between articular cartilage and subchondral bone, which exhibits major transitions in the composition and architecture of the cells and extracellular matrix. These features, which develop under the influence of morphogen gradients, enable the effective transmission of stresses during the articulation of joints. Here, I will introduce our new method of engineering highly integrated osteochondral tissue interfaces *in vitro*. This was achieved by designing and implementing an accessible benchtop approach for encoding morphogen gradients into biomaterials laden with multipotent stem cells.

METHODS: Density-driven phase separation was achieved by injecting a hydrogel precursor solution at a defined rate into another hydrogel precursor solution [2]. The latter solution was supplemented with a density modifier to enable the fluids to predictably demix into a gradient, which could then be encapsulated by triggered gelation. For osteochondral tissue engineering, both solutions contained gelatin methacryloyl (GelMA), human mesenchymal stem cells, and photoinitiator, while the base solution contained Ficoll as a density modifier and the injection solution contained bone morphogenetic protein 2 (BMP2) sequestered in heparin methacrylate (HepMA). The gradient fluid was crosslinked using UV irradiation and then cultured for 28 d in an osteochondral differentiation medium [3].

RESULTS: We designed and implemented a density-driven phase separation to generate polymer fluid gradients that could subsequently be encapsulated by gelation or polymerization. We used this method, requiring only a mold and a micropipette injector, to programme a range of gradients into common biomaterial systems. For the main application, we cast gradients of BMP2, sequestered with HepMA, into GelMA hydrogels containing human mesenchymal stem cells. Over 28 d, the sustained release of BMP2 triggered local osteogenesis and mineralization at one end of a cartilaginous tissue construct.

DISCUSSION & CONCLUSIONS: In this study, we used a fluid redistribution strategy to generate continuous osteoinductive gradients across an interface-free structure. Consequently, we were able to produce osteochondral tissue constructs with highly integrated zonal matrix, avoiding common issues with delamination or the exclusion of cells at the tissue interface. An interesting observation was the formation of mineralized tidemarks from hydrogels encoded with continuous morphogen gradients: an emergent structural feature that mimics natural developmental processes. We are now seeking to develop the complexity of this *in vitro* model by incorporating remote manipulation strategies to replicate other features of the osteochondral interface [4].

ACKNOWLEDGEMENTS: JPK Armstrong was supported by an Arthritis Research U.K. Foundation Fellowship (21138) and an MRC/ UKRI Innovation/Rutherford Fund Fellowship (MR/S00551X/1); C Li was supported by a Top University Strategic Alliance Ph.D. Scholarship from Taiwan; L Ouyang acknowledges support from the EPSRC (EP/P001114/1); MM Stevens acknowledges support from the grant from the U.K. Regenerative Medicine Platform "Acellular/Smart Materials—3D Architecture" (MR/R015651/1), an ERC Seventh Framework Programme Consolidator grant "Naturale CG" (616417), and a Wellcome Trust Senior Investigator Award (098411/Z/12/Z).

REFERENCES: [1] Li, Ouyang, Armstrong, Stevens "Advances in the fabrication of biomaterials for gradient tissue engineering" *Trends in Biotechnology* **2020**; [2] Li, Ouyang, Pence, Moore, Lin, Winter, Armstrong, Stevens "Buoyancy-driven gradients for biomaterial fabrication and tissue engineering" *Advanced Materials* **2019**. [3] Li, Armstrong, Pence, Kit-Anan, Puetzer, Correia Carreira, Moore, Stevens "Glycosylated superparamagnetic nanoparticle gradients for osteochondral tissue engineering" *Biomaterials* **2018**. [4] Armstrong, Stevens "Using remote fields for complex tissue engineering" *Trends in Biotechnology* **2020**.

Characterization of foam cell models using a label-free technique toward better atherosclerosis investigation

[1]Bowen Xie, [1]Wanjiku Njoroge, [2]Gianfelice Cinque, [1,3]Josep Sulé-Suso, [1]Ying Yang

[1]School of Pharmacy and Bioengineering, University of Keele, Stoke-on-Trent ST4 7QB, UK

[2]Diamond Light Source, Chilton Didcot OX11 0DE, UK

[3]University Hospital of North Midlands, Stoke-on-Trent ST4, UK

INTRODUCTION: Foam cell formation is triggered by the excessive influx of modified low-density lipoproteins (LDL), and the accumulation of cholesterol esters within the macrophages. Plaque progression is propagated by foam cells, which induce a cascade of inflammatory mediators that enhance lipoprotein retention, extracellular matrix modification and sustained chronic inflammation. Statins are commonly prescribed for the treatment of atherosclerosis. They function by lowering circulating LDL levels, and potentially initiating cholesterol efflux in foam cells. How statins initiate cholesterol efflux/reverse cholesterol transport (RCT), and the effect of statin dose and response time on RCT, requires a non-destructive characterization tool. In this work, we have assessed whether Synchrotron-based microFTIR spectroscopy of single cells can identify the lipid concentration in macrophages as atherosclerosis model, with and without statin treatment, using thin glass sample substrates.

METHODS: Murine macrophage cell line RAW264.7 was induced into M1 phenotype by treatment with 100ng/ml LPS and 100ng/ml IFN-γ, followed by stimulation with 100μg/ml LDL for 24h to generate foam cells. Foam cells were then incubated with atorvastatin at 0.6, 6, and 60μg/ml for 24h to investigate the effect on efflux of internalised lipid. Dynamic efflux was studied by incubating the foam cells with 6μg/ml atorvastatin for 24h, 48h, and 72h. The foam cells were cytospun and fixed onto microscope glass coverslips (24 x 50mm; 0.13–0.17mm thick). FTIR microspectra were analysed after acquisition via IR microscope (15x15 μm^2 slits) at MIRIAM beamline B22 of Diamond Light Source. Average 50 spectra per group were collected and analysed by PCA for the clustering via the QUASAR software (https://zenodo.org/record/4617978). Nitric oxide (NO) production was quantified using Griess assay, and absorbance read at 546nm. Media was collected 24h after stimulation with LPS (± IFN-γ, atorvastatin), IFN-γ (± LPS, atorvastatin), LDL (± atorvastatin). Lipid and nucleus were stained by Nile red DAPI for fluorescence imaging.

RESULTS:

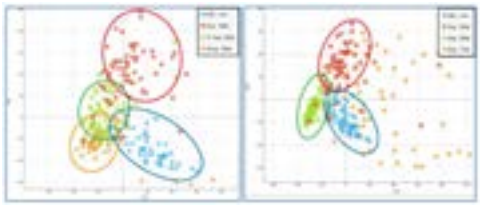

Fig. 1. *Left: Cells with atorvastatin at 0.6 (green), 6.0 (red), 60 μg /ml (orange) for 24 hours in comparison to control (blue). Right: Cells with atorvastatin at 6 μg /ml for 24-hour (red), 48-hour (green), 72-hour (orange) in comparison to control (no atorvastatin for 24 hour, blue). (Spectra, n=50)*

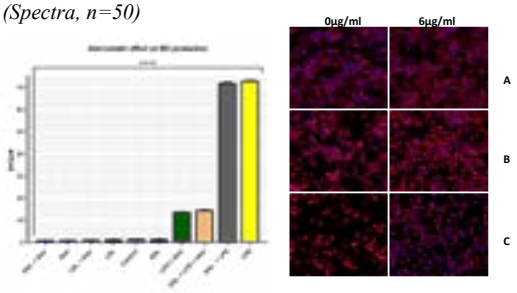

Fig. 2. *Left: atorvastatin effect on RAW264.7 NO production (n=5). Right: Atorvastatin (6μg/ml) effect on RAW264.7 RCT of LDL over 24h (A), 48h (B), 72h (C).*

DISCUSSION & CONCLUSIONS: The scatter plot (Fig. 1) shows very coherent spectral clusters via PCA unsupervised analysis on the cell groups treating with different atorvastatin dose and incubation time. Atorvastatin restricted foam cell NO production and triggered RCT over time (Fig. 2). FTIR single cell data correlates very well with biological assays, and can become a reliable, label-free technique to study atherosclerosis.

ACKNOWLEDGEMENTS: Diamond Light Source UK synchrotron radiation facility is acknowledged for beamtime SM27175.

Developing an estradiol-17β [E_2] responsive tissue engineered vaginal tissue model for evaluating biomaterials to be used in the female pelvic floor repair

S. Shafaat[1], S. MacNeil[1], V. Hearnden[1]

[1]*Department of Materials Science and Engineering, Kroto Research Institute, University of Sheffield, Sheffield S3 7HQ, United Kingdom.*

INTRODUCTION: Tissue engineered (TE) preclinical models of the vaginal epithelium and underlying tissue are needed for *in vitro* studies on vaginal pathogenesis, drug efficacy and irritability as well as the pathophysiology of sexually transmitted diseases. In this study a hormone-responsive, physiologically relevant, low cost and ethically sound model of the native vaginal tissues has been developed using sheep vaginal tissue. The long-term aim is to produce a model which can provide us with a better understanding of the interaction between vaginal tissue and biomaterials for the female pelvic floor repair.

METHODS: Decellularised sheep vaginal tissue (SVT) and primary sheep vaginal cells were used for the construction of TE vaginal models. Sheep vaginal tissues were decellularised using a detergent mix treatment (0.25% sodium deoxycholate and 0.5% tritonX 100) for 5 days and then seeded with primary vaginal epithelial cells and fibroblasts and cultured in the air-liquid interface (ALI) for upto three weeks.

The functionality of TE vaginal models was assessed by administration of estrogen (estradiol-17β [E_2]) into the culture medium and TE vaginal models were maintained for three weeks. Immunohistochemical analysis for the detection of Ki67 and cytokeratin 10 expression was performed to determine the effect of E_2 on vaginal epithelial cells proliferation and stratification.

RESULTS: Histological analysis (H & E staining) of the sheep vaginal tissue samples treated with the detergent mix revealed complete removal of epithelium and cellular components in tissue samples with adequate preservation of underlying extracellular matrix. Reconstructed vaginal tissue models showed structural similarities with the native vaginal tissue and cell metabolic activity remained for 14 days.

Our results showed a dose-dependent response of the TE vaginal epithelium to E_2. Higher E_2 concentrations showed an increase in epithelium thickness, stratification and an increase in proliferation of the cultured cells.

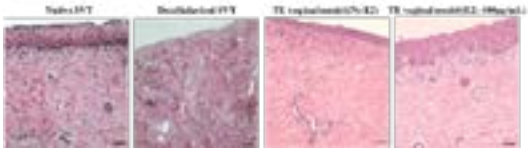

Fig. 1: Effect of estradiol-17β [E_2] on the TE sheep vaginal model epithelium thickness and stratification. Scale bar=100μm

DISCUSSION & CONCLUSIONS: Estradiol 17β- (E_2) promotes vaginal epithelial cell proliferation, stratification and cytodifferentiation by binding with estrogen receptor-α (ERα) in the human female urogenital tract. Our TE vaginal models have shown a similar response which provides us with a physiologically relevant hormone-responsive preclinical model that has potential applications in understanding the pathophysiology of vaginal diseases, drug discovery and research involving development of biomaterials for the female pelvic floor repair.

ACKNOWLEDGEMENTS: This work was funded by the University of Sheffield, Faculty of Engineering Post Graduate Research Committee (UPGRC) scholarship.

REFERENCES:

1. Zhang Y. et al. *Am. J. Transl. Res.* 2018; 10(11):3762–3772.

2. Orabi H. et al. *Transl. Res.* 2017; 180:22-36.

Acknowledgements

We would like to thank the University of Edinburgh, the School of Engineering for facilitating this event, without whose support this would not have been possible.

Thanks go to our local organising committee and the TCES Committee for their help in putting together a varied and topical programme and chairing the sessions. I thank our enthusiastic and hardworking team of moderators for their tremendous effort in the preparation and daily organisation of the virtual conference.

We are all grateful to our sponsors for generous funding, active participation in the sessions and contribution of talks.

Special thanks go to our core organisational team of Diane Reid, Emily Martin, Katrina Saridakis, Eddie Dubourg, Laura Smith and Karen Brocklehurst from the University of Edinburgh, School of Engineering without whose hard work, strong IT and organisational skills the event would not have been possible.

Finally, very special thanks to all our speakers for their contributions and innovations, in particular our invited key note speakers:

Professor Fergal O'Brien - Royal College of Surgeons in Ireland

Professor Kareen Coulombe - Brown University

Professor Molly Stevens – Imperial College London

Professor Brendan Harley - University of Illinois at Urbana-Champaign

Professor Liesbet Geris - University of Liège and KU Leuven

Dr Christine Horejs - Chief Editor, Nature Reviews Materials

Professor Jonathan Fallowfield - University Of Edinburgh

Mar sin leibh,
agus chi sinn sibh an ath bhliadhn!
(Scots Gaelic)

Farewell, see you all next year!